REMOTE SENSING OF EROSION AND SHALLOW WATER BATHYMETRY TO AID RIVER NAVIGATION ON THE COLVILLE RIVER, NUIQSUT AK

By

Cole S. Payne, B.S.

A Thesis Submitted in Partial Fulfillment of the Requirements

for the Degree of

Master of Science

in

Geology: Remote Sensing

University of Alaska Fairbanks

August 2018

APPROVED:

Santosh Panda, Committee Co-Chair
Anupma Prakash, Committee Co-Chair
Todd Brinkman, Committee Member
Paul McCarthy, Chair
Department of Geosciences
Leah Berman, Interim Dean
College of Natural Science and Mathematics
Michael Castellini, *Dean of the Graduate School*

ABSTRACT

The Colville is the longest river (~600 km) in Arctic Alaska. Nuiqsut is an established Alaska Native community of ~400 people on the Colville River. Its residents rely heavily on the Colville for subsistence needs, however, changing river dynamics caused by accelerated bank erosion, river siltation, low water, and shifting and drying channels are causing concern and making boat travel increasingly difficult and dangerous. Recently, local residents have reported increased erosion at bluff sites along the Colville, which threatens existing infrastructure. Also reported are unexpected shallow water sections along the main channel of the Colville, limiting their access to subsistence food sources. Residents have expressed a need for monitoring erosional rates on the Colville as well as a map product that could aid in river navigation.

These concerns shaped the main goals of this Thesis:

1) To use remote sensing techniques to map and quantify erosion rates and the volume of land loss at selected bluff sites along the main channel of the Colville, and to assess the suitability of automated methods of regional erosion monitoring
2) To use optical satellite images for mapping river bathymetry and generate GIS map products that show potential shallow water sections (<2m) and poor channel connections, and to assess the feasibility of future monitoring based off our methods that rely on extracting relative water depth values from publicly available optical remote sensing images.

For our erosional study we used orthomosaics from high resolution aerial photos acquired in 1955 and 1979/1982, as well as high resolution WorldView-2 images from 2015 to quantify long-term erosion rates and the cubic volume of erosion. We found that, at the selected sites, erosion rates averaged 1 to 3.5 m per year. The erosion rate remained the same at one site and increased from 1955 to 2015 at two of the four sites. We estimated the volume of land loss to be in the magnitude of 166,000 m^3 to 2.5 million m^3 at our largest site. We also found that estimates of erosion were comparable for manual hand-digitized and automated methods, suggesting our automated method was effective and can be extended to monitor erosion at other sites along river systems that are bordered by bluffs.

For our bathymetry study we used summer 2017 scenes from three optical sensors (PlanetScope 3m, Sentinel 2 10m, and Landsat 30m) along with field measurements on the river to map shallow water bathymetry along a 45 km stretch of the Colville. We found a strong correlation (R^2=0.89) between field-measured water depths and image-derived reflectance quantity (natural log ratio of green over red bands). We analyzed the two essential criteria for suitable bathymetry mapping from optical images: clear weather and clear water conditions. We expect several days (≈16) of suitable conditions during the ice-free season to facilitate reliable bathymetry mapping and remote monitoring of shallow water sites. We also discuss a relative depth mapping technique which is useful for boat navigation in the absence of ground truth measurements. We deliberately employed simple and robust empirical techniques that could serve as a basis for a fully developed river monitoring project in the near future led by local community residents. An implementation of our methods by the community, in order to develop a river depth monitoring program, would be an important step forward for the advancement of community-based science and the co-production of knowledge. Our technique may help address emerging environmental and societal issues in other regions where sufficient river navigation fosters local livelihoods.

TABLE OF CONTENTS

LIST OF FIGURES

Page

LIST OF TABLES

Page

ACKNOWLEDGEMENTS

A special thanks to everyone at UAF who has supported my degree and thesis work, especially my committee members: Santosh Panda, Anupma Prakash, and Todd Brinkman. Thanks to the community of Nuiqsut for welcoming our research into their community, especially Frederick Tukle Sr. for assisting with our field work. A big thank you to my wife Hannah, who supported me throughout my grad career while also pursuing her degree. Lastly thank you to my funding sources: Alaska EPSCoR Award #OIA-1208927, the state of Alaska, Alaska Space Grant, and the UAF Center for Global Change Grant.

Chapter 1

INTRODUCTION

1.1. Background

Native Alaskan villages need a new way to monitor their resources. For thousands of years Traditional Ecological Knowledge (TEK) has helped shape the way these communities change and adapt their resource management. However, in today's environment some of these resources are changing faster than ever which creates stress for TEK to keep up. One such resource is the rivers of Northern Alaska. These rivers serve as the transportation artery in a region with virtually no roads. Because of this, climate impacts on river geomorphic processes are particularly relevant to residents of river communities with mixed cash-subsistence economies, who heavily rely on the river for: recreation, visiting traditional family sites, and most importantly, access to their subsistence food sources that Northern Alaskan communities so heavily depend on (BurnSilver et al. 2016).

Subsistence harvesters within the Arctic region have expressed concern that changes in the environment are influencing their ability to move across landscapes and access traditional hunting, fishing, and gathering areas. Despite a sufficient natural-resource base in most areas, problems with access are a frequently expressed concern in many parts of the world where communities are trying to adapt to climate change and rely on local ecosystem services (Brinkman et al. 2016, Porter et al. 2014). Concerns such as increased erosion and shallow water create access issues for the users of these rivers. Decisions and policies need to be made in order to address these access issues for Northern Alaskan Communities. Unfortunately in today's climate environment TEK alone isn't always enough to sway decision and policy making (Nadasdy 1999). This is where a form of resource monitoring through the use of remote sensing can come into play.

Remote sensing has become a critical tool for monitoring natural resources by government agencies, conservation organizations, and private industry (Kennedy et al. 2009, Gross et al. 2009, Philipson and Lindell 2003, Stow et al. 2005). An emerging theme in the design and implementation of remote sensing based resource monitoring projects is the process of

stakeholder engagement by which scientists and stakeholders work together closely in an iterative relationship (Kennedy et al. 2009).

One aspect less discussed in literature is the effort to design remote sensing resource monitoring projects not only to be run by scientists, but be simple and robust enough to be undertaken by the communities themselves. This thesis aims to advance research to fill that gap by creating resource monitoring techniques and workflows that could potentially be repeated in the future by a non-technical community member in order to start cataloging changes over time. Involving the communities at this level creates a sustainable method for long term monitoring and change analysis that just can't be supported by scientific research projects alone. No one cares more about the resources being monitored than the users of the resource in question. Enabling stakeholders to study their own resources using conventional science techniques along with their own TEK gives them the best knowledge and opportunity to manage and plan for their future.

1.2. Thesis Objectives

This thesis uses remote sensing to examine multiple aspects relating to river access for the Colville River in Northern Alaska. Our work focuses on the small native village of Nuiqsut, which sits along the Colville. The aims of this thesis are to use community observations to guide our research questions, as well as our focused study sites, and arm the communities with scientific methods to help monitor the river, which can further help with decision making and validation of our results.

This thesis was designed from the beginning to include the concerns voiced by the community of Nuiqsut in all steps of the scientific process, from project design, field work, and ultimately result in an easily repeatable product capable of monitoring changing conditions on the Colville. We compiled the community concerns through multiple means including literature review of past work in Nuiqsut, speaking to other researchers working with the community, attendance and discussion at meetings with Nuiqsut community leaders, visits to Nuiqsut, and speaking directly with residents about their experiences.

One of the first things we learned was that residents travel great distances on the river—from Umiat to the Beaufort Sea—for subsistence hunting. Food security is an issue in Nuiqsut. More than 50% of surveyed households reported that they were unable to get enough subsistence food and 25% of households reported that at times they did not have enough food to eat (Brubaker, 2014).

Recently, residents of Nuiqsut have noticed accelerated changes in the river environment. Residents report bank erosion both in the village, which threatens infrastructure, and throughout the river system. Also, reported are shallow water conditions and drying tributaries that interfere with travel, damage boat engines, create hazards, and raise concerns about fish migration (Brubaker et al. 2014).

The Colville is not a one channel river. It is a braided river often with multiple channels to choose from. The issue for subsistence travelers is choosing the right channel when trying to reach their hunting grounds. If a traveler chooses to go down a channel that is too shallow it can damage their boat propeller, which is a costly problem as well as a dangerous one if it leaves the boat and its passengers stranded. Residents report difficulty in navigating the river which has resulted in limited access to harvest sites upstream. Residents used to boat upstream up to Umiat (~90 miles away) and go on the Chandler River for moose hunting. A good fishing creek near town is no longer suitable for travel due to low water; erosion has led to rapid drainage and sedimentation (*resident: Archie Ahkiviana*). Understanding the Colville River dynamics and its impact on river navigability is important for food security, safety, and mental health of Nuiqsut residents.

The goal of this research is to study erosion and shallow water conditions along the Colville River using high-resolution remotely sensed data. This research addresses the following key questions related to river navigability issues.

Question 1:

Has erosion on the Colville been accelerating in recent years like residents believe, and if so, where are these sites of accelerated erosion and how much sediment has been eroded into the river?

Objectives: For the selected stretch of the Colville River,

1. Map and estimate erosion rates and volume of land loss at selected bluff sites along the main channel of the Colville River from aerial photos and satellite imagery.

2. Assess the suitability of automated methods for regional erosion monitoring by comparing mapping results and land volume loss estimates from automated change detection methods and from hand-digitized measurements.

Question 1 and objectives 1 and 2 are discussed in thesis Chapter 2.

Question 2:

Where has the river gotten shallower over the years, and how could a remote sensing based depth product be useful for boat navigation?

Objectives: For the selected stretch of the Colville River,

3. Use digital image processing to estimate and map river bathymetry (water depth).

4. Produce GIS map products showing potential shallow water sections, sites of accelerated erosion, and poor channel connections, to aid river navigation.

5. Outline a simple and robust method for mapping river bathymetry for potential continued monitoring.

Question 2 and objectives 3, 4, and 5 are discussed in thesis Chapter 3.

Answering these questions and completing the research objectives serves twofold. First and most importantly it addresses real issues the community of Nuiqsut is facing. This study informs residents about the river and helps validate some of the changes they are documenting with TEK by means of western science. The second thing this thesis accomplishes is to create a framework for other studies that may wish to integrate TEK and science together in order to not only advance science but help communities make more informed decisions about their resources. The techniques outlined in the following pages are deliberately made to be robust and easily repeatable. This is done in order to enable non-scientists from Nuiqsut with basic knowledge of GIS, Remote Sensing, and limited resources the opportunity for continued monitoring and a better understanding of the river as a whole. This thesis pushes the idea of not only doing

scientific research alongside native communities, but giving the communities the tools to do the research themselves. In this way it helps advance existing literature on community involved research and provides guidance to future projects of similar merit.

1.3. Study Area

The Colville is the longest river in the Alaskan North Slope with a course of 600 km. It is also the largest river basin (53,000 km^2) north of the Brooks Range in Arctic Alaska. The river drains the North side of the Brooks Range and winds its way into a 550 km^2 delta 250 km east of the community of Utqiagvik (formerly Barrow) before emptying into the Arctic Ocean (Arnborg et al. 1966). We chose to study this river because of its significance to Nuiqsut, a Native village located on the Colville River about 25km South (upstream) from the Arctic Ocean. Residents use the Colville to travel from Umiat to the Beaufort Sea—for subsistence hunting. For this thesis we chose to study a 45 km stretch of the Colville. This stretch runs from the Village of Nuiqsut and heads south (upstream) past Ocean Point. Residents frequent this section of the river to reach moose and caribou hunting grounds.

The Colville serves as the Eastern border for the National Petroleum Reserve in Alaska (NPRA) which means that our study area also falls within the NPRA and subsequently has been geologically observed and summarized extensively since the early 1900's (Frederiksen et al. 1987). The regional geology of the North Slope of Alaska has been summarized in numerous papers (Gryc et al. 1969, Morgridge and Smith 1972, Detterman 1973, Jamison et al. 1980, Carmen and Hardwick, 1983, Bird 1985). The North Slope of Alaska is broken into multiple regions with our study area being within the Arctic Coastal Plain (ACP). The ACP stretches along the coast of the Arctic Ocean from Cape Beaufort in the West to the Canadian border on the East. The ACP is a flat featureless plain with thousands of oriented and unoriented lakes and drained lake basins (Black and Barksdale 1949). This region is underlain by continuous permafrost, perennially frozen ground, and is dominated by ice wedge polygons as well as other permafrost features (Black 1964).

Many large arctic rivers that flow south to north originate in non-permafrost zones. The Colville is unique in being one of the few large Arctic rivers that runs completely within a continuous permafrost zone. This is important because it limits geomorphic processes such as

runoff and groundwater discharge to a few short months of the ice-free season in late spring and summer (Walker and Hudson 2003). During this short summer season the geomorphological processes of the river are heavily controlled by permafrost. Thermal erosion and toe undercutting due to thawing permafrost along the river banks accounts for large chunks of land loss and erosion rates up to 3m per year in this region (Payne et al. 2018). During the first few weeks of breakup, usually between late May and mid-June, nearly 50% of annual discharge occurs (Walker et al. 1987) resulting in almost 75% of annual erosion and sediment load (Arnborg et al. 1966). Discharge and erosion decrease throughout the summer into early fall where temperatures remain consistently below freezing and the river freezes completely over.

The surficial geology of our study area is comprised mainly of Quaternary deposits as part of the larger Gubik formation that dominates the Arctic Coastal Plain. The term Gubik (which is believed to originate from the Eskimo name for the Colville River, Kupik) is used to describe all unconsolidated surficial materials overlying Cretaceous and Tertiary rocks in the ACP which were created by deposition (Leffingwell 1919). A vast majority of our study area, which encompasses the main channel of the Colville from Nuiqsut past Ocean Point, has stratified quaternary deposits of fine to medium sand, silty sand, and gravelly sand (Carter and Galloway 2005). The only exceptions we see to this are along the north banks of the Nigliq channel near Nuiqsut and along the western bank of Ocean Point near the southern end of our study area. The Nigliq channel is an offshoot of the main Colville that stems off near the village of Nuiqsut and heads to the Arctic Ocean along the west side of the Colville delta. It is a very important channel as it is used by Nuiqsut to reach the main Colville as well as the Arctic Ocean. Along the Nigliq we see banks of slightly finer grained deposits than the rest of our study area as well as deposits and bedding of cobble gravel due to erosion of larger fluvial deposits near the village of Nuiqsut (Carter and Galloway 2005). For this reason, the Nigliq channel is also used to dredge for gravel which helps build and maintain roads in Nuiqsut. The biggest geologic difference we see in our study area is along the high west bank bluffs of Ocean Point. This section exposes a Cretaceous non-marine sandstone, siltstone, and shale with minor coaly beds and thin tephra layers. This is one of the few places near our study area where we see non Quaternary deposits at the surface (Carter and Galloway 2005).

The climate of our study area is of great importance to this thesis due to the nature of our research and its relation to climate change. Our study area is in an Arctic region which is characterized by long winters with temperatures well below freezing for most of the year followed by short moderate summers. Most recently average yearly air temperatures near Nuiqsut range from around -8 to -9°C with average winter snow depths measuring around 20 cm (USGS Climate Data). Climate change particularly affects Arctic regions, as reported by Wendler et al. (2014) where a 2.7°C increase in average air temperature was seen across Arctic Alaska between 1979 and 2013, far greater than any other regional increase observed in Alaska. These results are also backed up by Payne et al. (2018) where climate data is analyzed from the USGS and shows significantly positive increases in average air temperature, ground temperature, and snow depth for three sites near our study area within the past two decades. The warming of the arctic has also affected length of the ice-free summer season for the Colville. It has been reported that these warming trends have caused a lengthening of the Arctic melt season at a rate of 4 to 5 days per decade since 1979 (Stroeve et al. 2014).

1.4. Thesis Outline

Chapter 1 provides the general background and introduces the research questions and objectives. It also introduces the study area and the structure of the thesis.

Chapter 2, entitled "Remote Sensing of Erosion on the Colville River, North Slope Alaska" is published in the Remote Sensing journal. It presents remote sensing techniques to examine the massive bank erosion over a 60 year period along selected bluffs on the Colville, which is a concern expressed by local residents. It also presents the suitability of automated method for regional erosion monitoring. By studying long term erosion rates on the river we can determine whether concerns of increased erosion are true and what that might mean for the community of Nuiqsut. Heavy river erosion creates many reasons for residents to be concerned including but not limited to, damage of infrastructure, loss of traditional sites, loss of fish habitat, and increased sediment load into the river system which can create shallow water and limit access to hunting and fishing sites. Having an idea of erosion patterns in the past can help the community of Nuiqsut in planning and decision making for their future.

Chapter 3 entitled "Remote Monitoring of Shallow Water Sites to Inform Boat Navigation on the Colville River, Alaska: A Feasibility Study" is being submitted to the Environmental Research Letters for publication. In this chapter we focus on calculating Colville river bathymetry from remote sensing using a common band ratio formula (Legleiter et al. 2009). We use these bathymetry calculations to map areas of shallow water on the river which is a common concern from Nuiqsut residents. In a landscape where roads are nonexistent, residents rely on the river for safe access to their traditional subsistence hunting and fishing sites. Recently residents have reported shallow water spots on the river which create hazardous conditions and inhibit access to subsistence sites. Issues relating to subsistence access have been identified as one of the key future concerns for Native Alaskan communities, even more so than subsistence resource abundance and seasonal availability (Brinkman et al. 2016). For future decision and policy making for Native Alaskan communities more attention needs to be focused on harvester's access to a resource, not just resource abundance. By studying a common river access issue (shallow water) we can enable Native Alaskan Communities to advance the subsistence policy discussion while contributing to the field of remote sensing of river bathymetry simultaneously.

Chapter 4 synthesizes the general finding from both chapters 2 and 3 and provides the larger framework of issues related to dynamics and navigability of a large Arctic river, its impacts on the local communities, and the feasibility of locally monitoring the river using simple remote sensing methods. The chapter also presents thoughts on future research directions stemming from this work.

Chapter 2

[1]Remote Sensing of River Erosion on the Colville River, North Slope Alaska[1]

Abstract

The Colville is an Arctic river in the Alaska North Slope. The residents of Nuiqsut rely heavily on the Colville for their subsistence needs. Increased erosion has been reported on the Colville, especially along bluffs, which shaped the goals of this study: to use remote sensing techniques to map and quantify erosion rates and the volume of land loss at selected bluff sites along the main channel of the Colville, and to assess the suitability of automated methods of regional erosion monitoring. We used orthomosaics from high resolution aerial photos acquired in 1955 and 1979/1982, as well as high resolution WorldView-2 images from 2015 to quantify long-term erosion rates and the cubic volume of erosion. We found that, at the selected sites, erosion rates averaged 1 to 3.5 m per year. The erosion rate remained the same at one site and increased from 1955 to 2015 at two of the four sites. We estimated the volume of land loss to be in the magnitude of 166,000 m^3 to 2.5 million m^3 at our largest site. We also found that estimates of erosion were comparable for manual hand-digitized and automated methods, suggesting our automated method was effective and can be extended to monitor erosion at other sites along river systems that are bordered by bluffs.

2.1. Introduction

Erosion plays a significant role in the changing environment of a river. It affects water flow, water quality, channel width and depth, and safe use of a river as a transportation corridor. In the Arctic, climate warming severely influences river geomorphic processes, including erosion, especially when a river runs through a continuous permafrost zone [1]. Warmer air and water temperatures lead to more pronounced thermal erosion and toe undercutting of ice-rich permafrost banks, resulting in erosion through massive block failures. This process is unique to rivers flowing through continuous permafrost and results in higher bank erosion rates with increasing bank height, which is uncommon for non-periglacial rivers [2].

[1] Article Published as: Payne C, Panda S, Prakash A. Remote Sensing of River Erosion on the Colville River, North Slope Alaska. Remote Sensing. 2018 Mar 5;10(3):397.9

The Colville River is frozen seven to eight months of the year, creating a very short ice-free season for intense erosion, transportation, and redeposition of sediment [3]. Climate impacts on river geomorphic processes are particularly relevant to residents of river communities with mixed cash-subsistence economies, who heavily rely on the river to access and harvest subsistence food [4]. There are two established Alaska Native communities along the Colville: Umiat and Nuiqsut. During our field visit we spoke with Nuiqsut residents about changes they perceive to the Colville River and the effects on the community. Residents reported accelerated erosion throughout the river system and difficulty in navigating the river, which has resulted in increasingly limited access to harvest sites upstream. Also, as part of a six-year study to understand social and ecological changes in Alaska and the ability of communities to adapt to those changes, Nuiqsut residents were asked "How has erosion changed along the Colville?". Of the interviewed residents, 61% reported more or faster erosion along the Colville River now than there used to be, and that increased erosion contributes to changes in the river environment; and 11% reported no change [5].

Some residents believe that the changes in the Colville River are happening due to recent climate warming. Wendler et al. [6] reported an average warming of 2.7 °C across Arctic Alaska from 1979 to 2013, which is far greater than that recorded during any other time period across Alaska as well as across other climate zones. Warmer ground and air temperatures caused earlier river breakups in recent years, leaving the river banks exposed to flowing water for longer periods [7]. Also, changes in seasonality are resulting in very intense and rapid seasonal changes to the Colville, such as lengthening of thawing season, and flooding during the spring snowmelt due to rapid warming [5]. Some studies on erosion in Northern Rivers [1] point to a possible correlation between climate warming and accelerated erosion. We will analyze air temperature, ground temperature, snow depth, and length of summer season data to verify if a similar trend also occurs in the Alaska North Slope, which may contribute to accelerated erosion along the Colville.

The focus of this paper is to investigate riverbank erosion at bluff bound sites of the Colville River using a simple yet robust approach that can be easily repeated on newer images. The goals of this study are (1) to map and estimate erosion rates and volume of land loss at selected bluff sites along the main channel of the Colville River from aerial photos and satellite imagery; and (2) to assess the suitability of automated methods for regional erosion monitoring

by comparing mapping results and land volume loss estimates from automated change detection methods and manual hand-digitized measurements. We do this by identifying four sites of heavy erosion and measuring erosion rates at those sites using aerial and satellite imagery from 1955, 1979, 1982, and 2015. We estimate the volume of land loss by using the mapped erosion area and terrain height from a high-resolution Arctic Digital Elevation Model (DEM), which employs a novel yet simple technique. For broader applicability of the research, we deliberately keep the processing approach simple, practical, and easy to repeat.

2.2. Study Area

The Colville is the longest river in the Alaskan North Slope with a course of 600 km. It drains into a 550 km^2 delta, 250 km east of the community of Utqiagvik (formerly Barrow). The Colville River serves as one of the transportation arteries in the North Slope of Alaska, a region with virtually no roads. We chose this river because of its significance to Nuiqsut, a Native village located on the Colville River about 25 km South (upstream) of the river mouth on the Beaufort Sea (Figure 2.1). Villagers travel great distances on the river, from Umiat to the Beaufort Sea, for subsistence hunting. They frequent this section of the river to reach moose and caribou hunting grounds.

We focused our study on the bluff bound parts of this frequently used section of the main channel of the Colville River. We used the main channel of the river to study erosion, as this is the primary navigation corridor and the larger channel size also makes it more appropriate for remote sensing-based mapping and investigation. We focused on bluff sites because extensive erosion usually occurs along bluffs [8–12]. Additionally, on nadir-looking remote sensing images, the sharp contrast between the tundra, the bluff face, and the river water is particularly suitable for delineating the water–land boundary, which is necessary to monitor erosion. We selected four bluff sites along the Colville (Figure 2.1) that suitably represent the variability of bluffs along the Colville. The bluff heights at these sites range from 5–33 m.

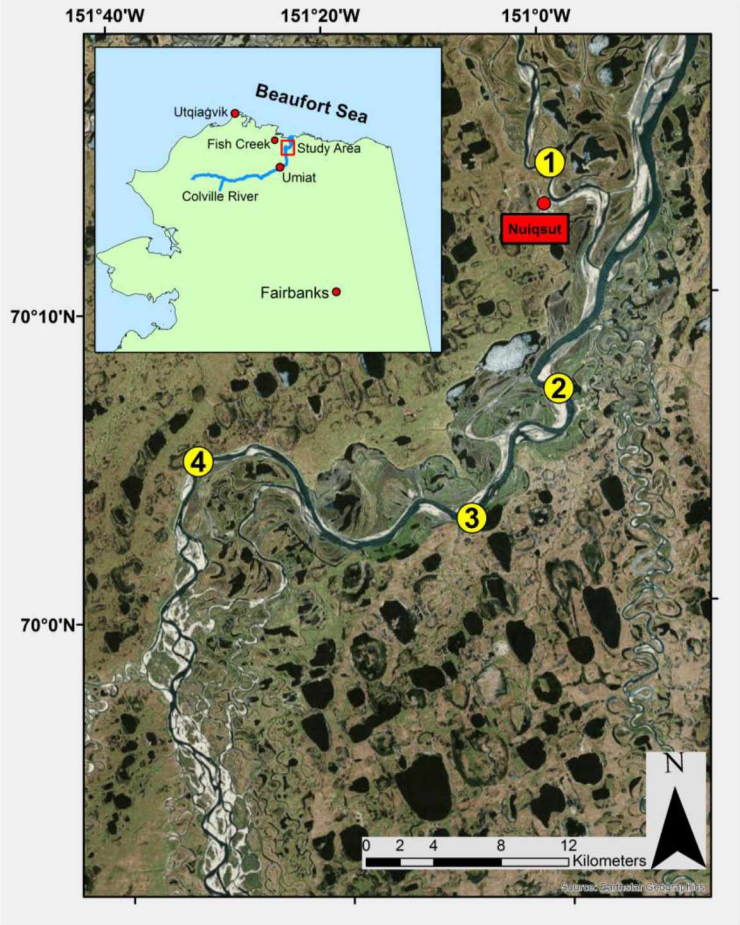

Figure 2.1. Study area map showing a stretch of the Colville near the village of Nuiqsut, Alaska (AK). The four sites of heavy erosion studied here are highlighted in yellow.

2.3. Data

2.3.1. Remote Sensing Data

This study focused primarily on the use of remote sensing data (Table 2.1) to study erosion at selected sites on the Colville over an extended time period (since 1955). These include orthomosaics of the study sites from 1955 and 1979/1982, accessed through the Alaska National Science Foundation Established Program to Stimulate Competitive Research (Alaska NSF EPSCoR) data catalog [13]. The 1955 orthomosaic has an effective spatial resolution of 2 m and was generated using black and white images that were acquired by the US Geological Survey (USGS) in an airborne mission in late July of that year. The 1979/1982 orthomosaic has an effective spatial resolution of 1.7 m and was generated using color infrared images that were acquired during two separate airborne campaigns flown as a part of the Alaska High Altitude

Aerial Photography mission. The southern half of the study area was imaged during the summer of 1979, while the northern half was imaged three years later in 1982. For the recent time period, we used a cloud-free WorldView-2 image from Digital Globe Inc. that had a spatial resolution of 1.4 m [14]. Together, these datasets covered a 60-year span (1955–2015), which is an ample amount of time to detect and study large-scale erosion along the river. For ease, in the remainder of this article we refer to the orthomosaics as images, as during the processing we treat them similar to any other satellite image.

We attempted to locate images for summers in the 2000–2010 time-frame to verify Nuiqsut residents' statements about accelerated erosion in recent years, but were unable to access cloud-free, high-resolution imagery for that period.

Another key piece of data is the Arctic Digital Elevation Model (ArcticDEM), accessed through the Polar Geospatial Center at the University of Minnesota [15]. We used this 5 m resolution model to estimate and quantify the volume of land loss from the river banks due to erosion.

Table 2.1. Details of remotely sensed data used in this study.

Data Type	Resolution	Time Period	Data Sources
USGS * North Slope Colville River Orthomosaic	**Panchromatic: 2 m**	**24 July 1955**	**GINA *, NSF *, Alaska EPSCoR ***
AHAP * North Slope Colville River Orthomosaic	**Color Infrared: 1.7 m**	**Summer 1979 and 1982**	**GINA, NSF, Alaska EPSCoR**
WorldView-2 satellite image	**Multispectral: 1.4 m**	**7 July 2015**	**DigitalGlobe Inc.**
ArcticDEM	**DEM: 5 m**	**2016**	**Polar Geospatial Center**
North Slope climate data		**1998–2016**	**USGS, Weather Underground**

USGS *: United States Geological Survey. AHAP *: Alaska High Altitude Aerial Photography. GINA *: Geographic Information Network of Alaska. EPSCoR *: Established Program to Stimulate Competitive Research. NSF *: National Science Foundation.

2.3.2. Climate Data

Local climate data was accessed through the USGS [16] and Weather Underground [17] websites. We used data from USGS weather stations located around the North Slope of Alaska dating back to 1998. The closest USGS station to Nuiqsut is Fish Creek, located about 40 km NW of Nuiqsut. There is also an Umiat USGS station. Data used from these weather stations included monthly averages of both ground and air temperatures, and snow depth. Annual average

air temperature data was also available for the village of Nuiqsut from the weather station located at their airstrip.

2.4. Methods

2.4.1. Mapping Erosion by Automated Digital Change Detection

Aerial and satellite images are commonly used to study river and coastal erosion [18]. For temporal monitoring and change detection, it is important to ensure that the different date images have minimal geolocation errors [19]. As mentioned above, we used images from three different time points to study the change over six decades in our study area. The images from 1955 and 1979/1982 were already orthorectified; however, by inspection we found that the geolocation accuracy of these products was off by 4 to 10 m in some places, which was not optimal for our change analysis. For better geolocation accuracy and to reduce misregistration amongst the images we used the 2015 WorldView-2 image as the master/base image and carried out an image-to-image coregistration using tie-points and a first order affine transformation (Figure 2.2). There were no man-made features on our 1955 image (Nuiqsut village was established in 1974), therefore we used lakes that looked similar between the 1955, 1979/1982, and 2015 images and had a distinguishing feature, such as a jutting peninsula or unique shoreline shape, that could be used as a tie-point. Since there is no way to definitively ascertain the depth of these lakes in the images, a relative water depth analysis was performed between the different years. For this analysis, we chose the lakes to be used as tie points, then measured between two distinguishable features across the same lake in different years. We assumed that lower water would mean a shorter distance between these two shore points and higher water, a farther distance. If a lake had a similar distance between features in both 2015 and earlier dates images, it was used as a tie point. Image-to-image coregistration resulted in the temporal images aligning with an accuracy of 2 m or less, as confirmed by verifying the locations and boundaries of 20 lakes around each study site. Pixel sizes of air photos and images used in this study ranged from 1.4 to 2 m, so a 2 m offset represented 1.5 pixels or less of registration error. This was an acceptable registration error for this study. Rather than resampling all the images to the same pixel size, we decided to keep the original pixel sizes. The small 0.6 m of difference between the 1955 and 2015 image resolutions contributed a negligible amount of error to the land cover mapping.

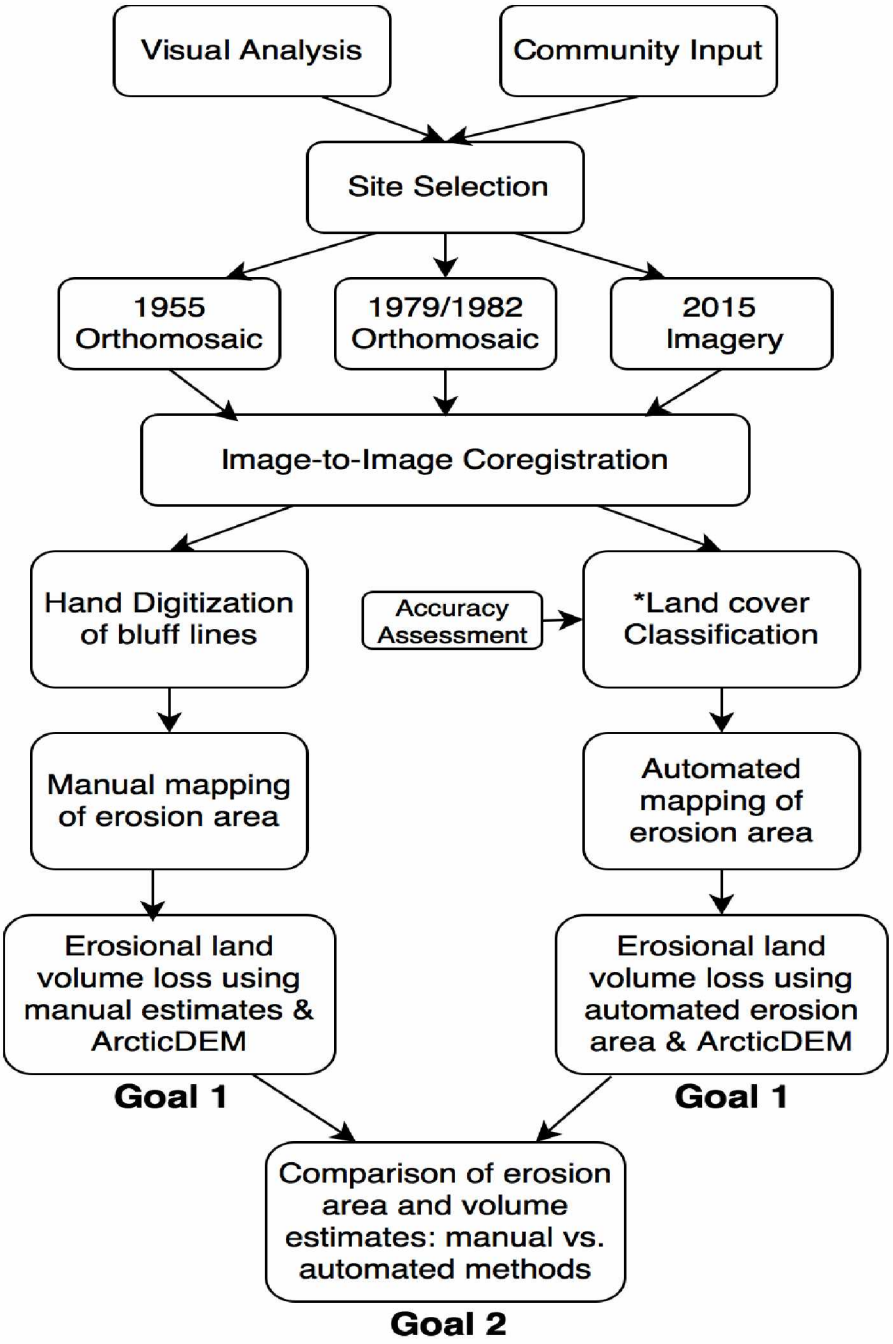

Figure 2.2. A flowchart showing the data processing steps from site selection to erosion area and land loss volume estimation.*Land cover classification was performed using a maximum likelihood classifier on the 1979, 1982, and 2015 datasets; whereas, land cover classes (land and water) were manually digitized from the 1955 dataset.

We then performed a supervised classification using a maximum likelihood classifier on three (1979, 1982, and 2015) of the four images, generating three output classes: water, bare

ground or sandbar, and tundra. We deliberately limited the number of classes because these were the three minimum classes needed in order to characterize either erosion or deposition. We chose to use a maximum likelihood classifier (MLC) because it can readily accommodate covarying data, a common occurrence with satellite image data, and MLC's have been proven to perform well over a range of cover types, conditions, and sensing systems [20–23] Also, the fact that maximum likelihood is one of the most popular classifiers, simple to use, and readily available with free GIS platforms was important to us for potential future erosion monitoring by someone with limited resources.

The 1955 image was a single band panchromatic image. The signature of land cover features, such as tundra, sand bars, and the river, were similar enough that we could not satisfactorily map land cover using a digital classifier. Instead, we mapped the river channel through visual interpretation and manual digitization [24]. The digital signatures of bare ground (bluffs and sandbars) and shrub tundra were very similar in the 1955 panchromatic image, therefore we could not differentiate between the two. This gave us only two land cover classes (water, or land) for the 1955 panchromatic image. Land cover in the remaining images (1979/1982, and 2015) was separated into three classes: water, bare ground or sandbar, and tundra.

Upon completing the classification, we performed an accuracy assessment on each of the classified images [25]. We generated a total of 90 random points, 30 for each class. We then compared the land cover maps to the actual images at these random points and marked them as either matching the correct land cover type or not. Land cover classes were easy to identify on a standard false color composite of near infrared, red, and green bands, displayed in red, green, and blue respectively. Once these points were analyzed, we estimated percentages of overall accuracy based on how many points were correctly classified. User and producer accuracies were also calculated for each class (Table 2.2). Our 1955 image was hand-digitized and not classified like the others, therefore no accuracy assessment was performed. As seen in Table 2.2, each of the three images had near or above 95% overall classification accuracy and a Kappa value above 0.9, which ensures high confidence mapping the erosion area.

Table 2.2. Accuracy assessment table showing user, producer, overall accuracy, and the Kappa Coefficient for each of the three classified images.

Classification Accuracy	**1979**		**1982**		**2015**	
	User's Accuracy	Producer's Accuracy	User's Accuracy	Producer's Accuracy	User's Accuracy	Producer's Accuracy
Water	**96.7%**	**93.5%**	**100.0%**	**90.9%**	**100.0%**	**90.9%**
Bare Ground/Sandbar	**86.7%**	**100.0%**	**96.7%**	**96.7%**	**90.0%**	**100.0%**
Tundra	**100.0%**	**90.9%**	**90.0%**	**100.0%**	**100.0%**	**100.0%**
Overall Accuracy	**94.4%**		**95.6%**		**96.7%**	
Kappa Coefficient	**0.92**		**0.94**		**0.96**	

After the accuracy assessment, a digital change detection was performed to identify areas of high erosion or deposition. Each of the three classes from each image was given a unique numerical value. Then, simple band math was performed by multiplying land cover classification images by each other for two different time periods (Figure 2.3) [26]. This gave a new classified image with nine unique values: three represented no change in land cover type between images; three represented erosion between images shown as either tundra changing to water, tundra changing to bare ground or sandbar, or bare ground or sandbar changing to water; and one outcome represented deposition, i.e., water changing to bare ground or sandbar. The final two outcomes were ignored as they represented water or sandbars turning back into tundra, a scenario which did not take place in this river system over this time scale. Figure 2.3 shows the classification values for 1979 and 2015 and the resulting table created by multiplying the two classification images. These nine results represented one of four possibilities, as listed at the bottom of the figure.

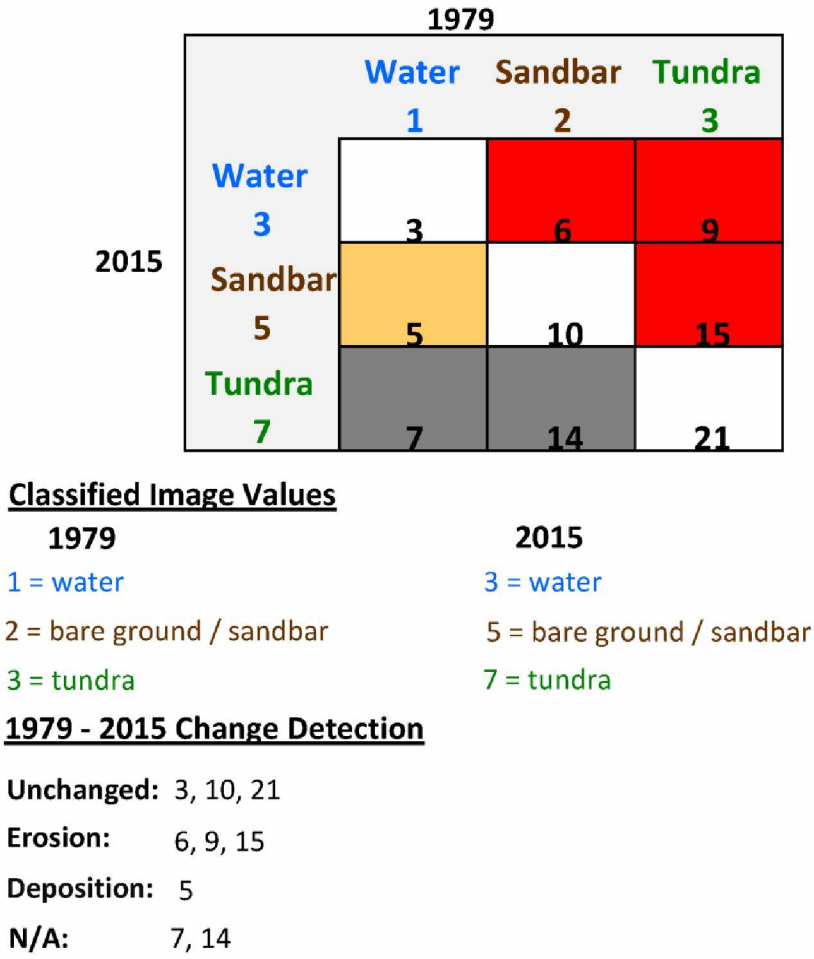

Figure 2.3. Multiplying classified images by each other, resulting in values that represent different scenarios between 1979 and 2015.

2.4.2. Mapping Erosion by Manual Hand-Digitization

In the absence of field measurements, visual interpretation and manual digitization of bluff lines is the only logical approach to assess the accuracy of erosion area estimates from the automated digital change detection method. At the study sites, the river water abuts bluff faces. The simplicity of this land cover lends itself well to accurate mapping of the tundra–bluff and bluff–water boundaries using manual digitization based on visual interpretation.

We manually digitized the bluff lines at the four erosion sites for the years 1955, 1979/1982, and 2015. The digitizing was performed directly on the original images, not on the classified or change detection images (Figure 2.2). For this study, "bluff line" was defined as the line where tundra can easily be distinguished from either water or sandbar. Using a tundra line on a cliff as our reference point for mapping bluff line erosion eliminates any discrepancies caused by

changing water height between images that might cover or uncover patches of sandbar along the banks of the river.

After bluff lines were digitized for the three time periods, we estimated erosion using two measurements. Average erosion between images was calculated by sampling evenly across the digitized shorelines (using 15 transects) and by measuring the perpendicular distance from one year's bluff line to the next. This was calculated three times for each site: between the bluff lines of 1955 and 1979/1982; 1979/1982 and 2015; and 1955 and 2015. The distance in meters between river bluff lines from different years gave us an erosional distance as well as a timespan, which was converted to an average erosion rate expressed as meters per year (m/year). Then, we estimated the maximum erosion rate at each site using only the transect of greatest value for each year. This maximum distance was also converted to erosion rate in m/year.

2.4.3. Estimating the Volume of Land Loss

We calculated the cubic volume of land loss due to erosion by measuring the area of our four erosion sites and multiplying that by an average height based on current DEM values. We created vector polygons of the eroded sites based off the bluff lines digitized in the previous step. These polygons represent all of the erosion between 1955–1979/1982, 1979/1982–2015, and 1955–2015 for each site. We then calculated the area of these polygons in square meters.

Elevation data for the 1955 and 1979/1982 bluff lines did not exist for our study sites. We also could not find any published methods to estimate paleo bluff line elevations that could be applied to decadal-scale change detection. To estimate bluff line elevations, we assumed that the current trajectory of changes in elevation and slope across a site reflected the trajectory of changes across the same site in the past. For each site, we plotted five transects across the available DEM: four perpendicular to the shoreline and a fifth running parallel along the whole erosion site (Figure 2.4). These five transects were plotted to show elevation changes. The average of all five transects was taken and used as the height value, in order to calculate cubic volume loss at all erosional sites with a simple formula:

$$\boldsymbol{V = A \times h}$$

V: volume of land loss in m^3; A: area of erosion in m^2; h: bluff height in m).

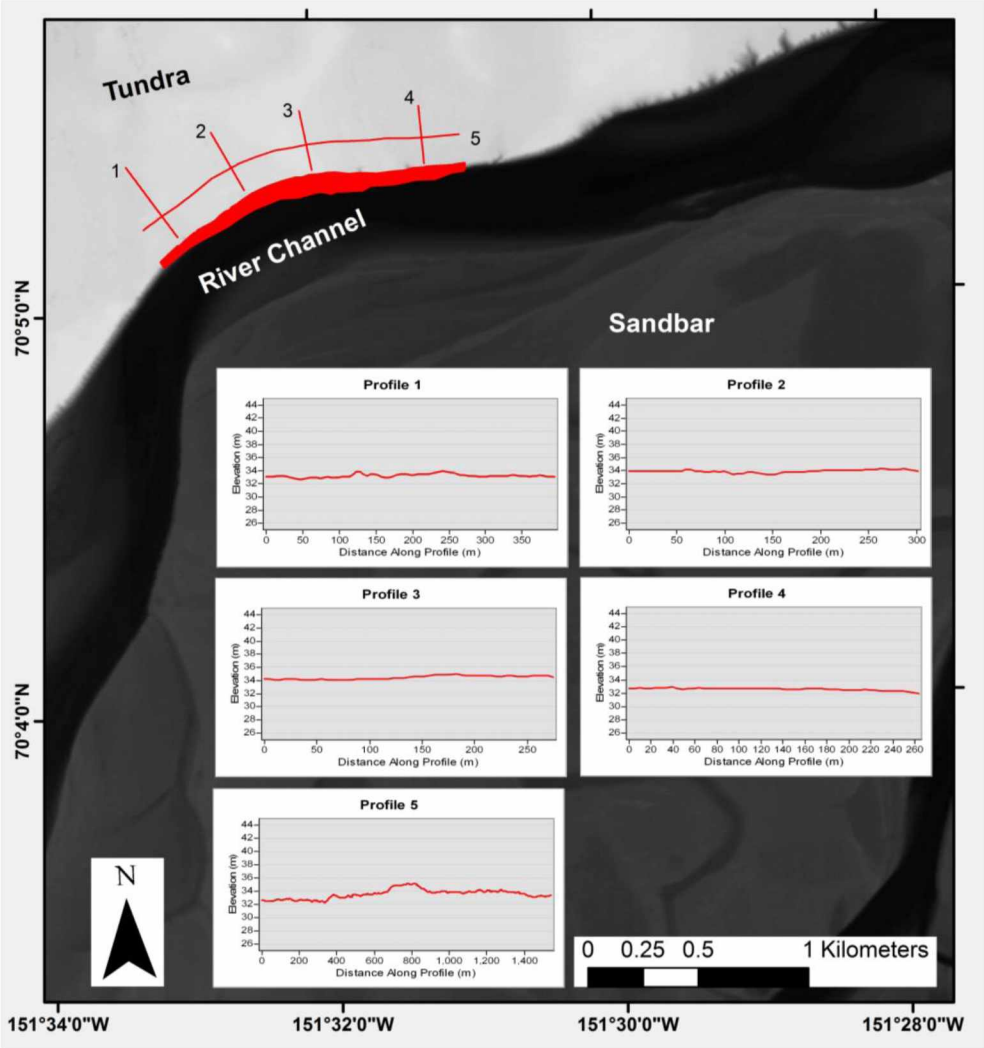

Figure 2.4. ArcticDEM at Site 4, showing the digitized erosion area from 1955–2015 (red polygon). The five lines represent transects taken across DEM, in order to calculate the average height of tundra for erosional volume loss estimates. The four overlaid graphs show the profiles of each transect.

2.4.4. Analysis of Climate Data

We analyzed the annual averages of ground and air temperature and snow depth for the Umiat and Fish Creek sites, and air temperature data from Nuiqsut, to determine any trends in the data and to see if any such trends were statistically significant at a confidence level of 95%. We wanted to learn and report the degree of climate warming and changes in snow cover near the study area because previous studies on Arctic river erosion have identified warming air temperature and increased snow cover as among the drivers of riverbank erosion [1,12].

2.5. Results

2.5.1. Mapping Erosion Results

Figure 2.5 shows the classified map of Site 1, derived from the 2015 WorldView-2 image. The main river channel can easily be distinguished, as can sandbars along the river and the surrounding tundra. The grid-like feature in the bottom center of the image is the village of Nuiqsut. For our classification, roads and buildings most closely resembled bare ground/sandbar and were classified as such. The smaller blue shapes in the tundra are the lakes that litter the North Slope.

Figure 2.6 shows the areas of heavy erosion near Site 1 between 1955 and 2015. As expected, we see erosion, in red, along the outer bank of the river bends. Also, shown in green is the sandbar migration further into the river channel, representing deposition of sand from upstream.

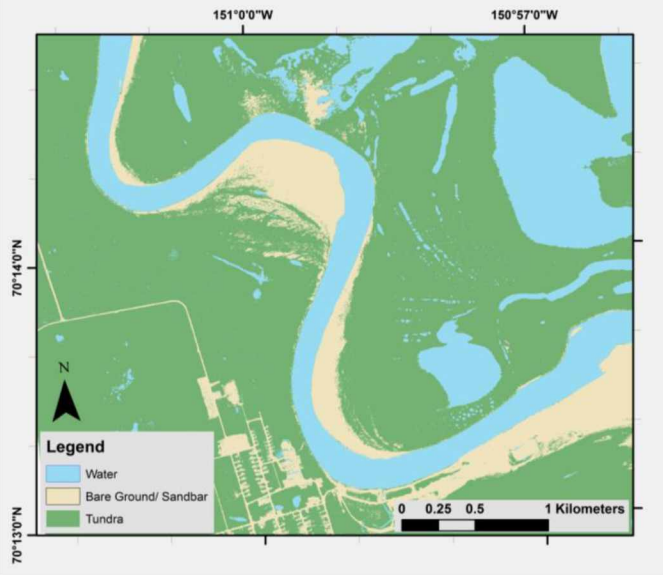

Figure 2.5. Land cover classification map of Site 1, processed from the 2015 WorldView-2 image using the maximum likelihood supervised classification method.

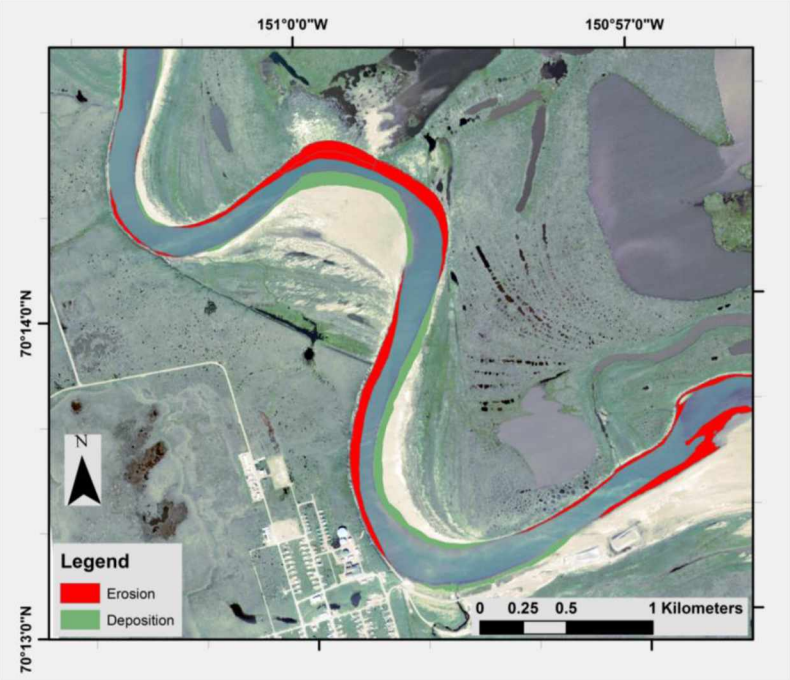

Figure 2.6. A change detection layer highlighting erosion and deposition at Site 1 from 1955 to 2015 overlaid on the 2015 WorldView-2 image.

2.5.2. Volume of Land Loss Results

The measured erosion distances and calculated erosion rates for each of the four study sites (Table 2.3) were based on the hand-digitized bluff lines generated in this study. In Table 2.3, the second column from the right shows the cubic volume of erosion calculated from the automated digital change detection method without any input from the user. The percentage of error is shown for each of the cubic volume calculations performed using the digital change detection method. This error value represents the difference in estimation compared to the hand-digitized bluff lines and calculations, which are assumed to be as accurate as possible. A small percentage of error indicates that the automated method can be used as an acceptable substitute for mapping river erosion over large areas where hand-digitization and calculation are unfeasible.

Table 2.3. Average and maximum erosion distances and rates for each site over our three time periods, expressed in meters and m/year, as well as the area of each erosion site between 1955 and 2015, with estimated cubic volume loss based on DEM.

Erosional Rates and Volume Estimations

Site	Years	Avg. Erosion Distance (m)	Avg. Erosion Rate (m/year)	Max. Erosion Distance (m)	Max. Erosion Rate (m/year)	Erosion Area, Hand-Digitized Calculation (m^2)	Erosion Area, Change Detection Calculation (m^2)	Cubic Volume of Erosion, Hand-Digitized (m^3)	Cubic Volume of Erosion, Change Detection (m^3)	% Error Change Detection vs. Hand-Digitized
1								**Average Elevation: 5.04 m**		
	1955–1982	**43**	**1.59**	**56**	**2.07**	**25,085**	**24,571**	**126,428**	**123,838**	2.05%
	1982–2015	**52**	**1.58**	**61**	**1.85**	**31,959**	**31,819**	**161,073**	**160,368**	0.44%
	1955–2015	**95**	**1.58**	**117**	**1.95**	**57,044**	**57,411**	**287,502**	**289,351**	0.64%
2								**Average Elevation: 5.63 m**		
	1955–1979	**29**	**1.21**	**37**	**1.54**	**14,845**	**12,954**	**83,577**	**72,931**	12.74%
	1979–2015	**32**	**0.89**	**37**	**1.03**	**14,747**	**16,555**	**83,026**	**93,205**	12.26%
	1955–2015	**61**	**1.02**	**68**	**1.13**	**29,592**	**26,866**	**166,603**	**151,256**	9.21%
3								**Average Elevation: 7.51 m**		
	1955–1979	**42**	**1.78**	**66**	**2.75**	**51,714**	**53,626**	**388,372**	**402,731**	3.70%
	1979–2015	**78**	**2.17**	**125**	**3.47**	**97,843**	**100,907**	**734,801**	**757,812**	3.13%
	1955–2015	**120**	**2**	**180**	**3**	**149,557**	**156,396**	**1,123,173**	**1,174,534**	4.57%
4								**Average Elevation: 33.56 m**		
	1955–1979	**16**	**0.67**	**33**	**1.38**	**23,884**	**25,381**	**801,547**	**851,786**	6.27%
	1979–2015	**38**	**1.06**	**53**	**1.47**	**50,352**	**47,877**	**1,689,813**	**1,606,752**	4.92%
	1955–2015	**54**	**0.9**	**87**	**1.45**	**74,236**	**72,889**	**2,491,360**	**2,446,155**	1.81%

As seen in Table 2.3, Sites 3 and 4 showed increased erosional rates and cubic volume loss since 1979, while Site 1 remained relatively constant over the entire timespan. Site 2 was the only site that showed a slowing down in erosion rate. It is worth noting that Sites 1, 3, and 4 were all located on bends in the river; whereas, Site 2 was along a straight portion of the channel.

For each site, we calculated the average erosion rate for the time periods 1955–1979/1982 and 1979/1982–2015, as well as for the whole period, from 1955 to 2015 (Figure 2.7). Erosion rates for the 1979/1982–2015 period were either equal to or greater than the 1955–1979/1982 and 1955–2015 erosion rates at three of our four sites (Table 2.3).

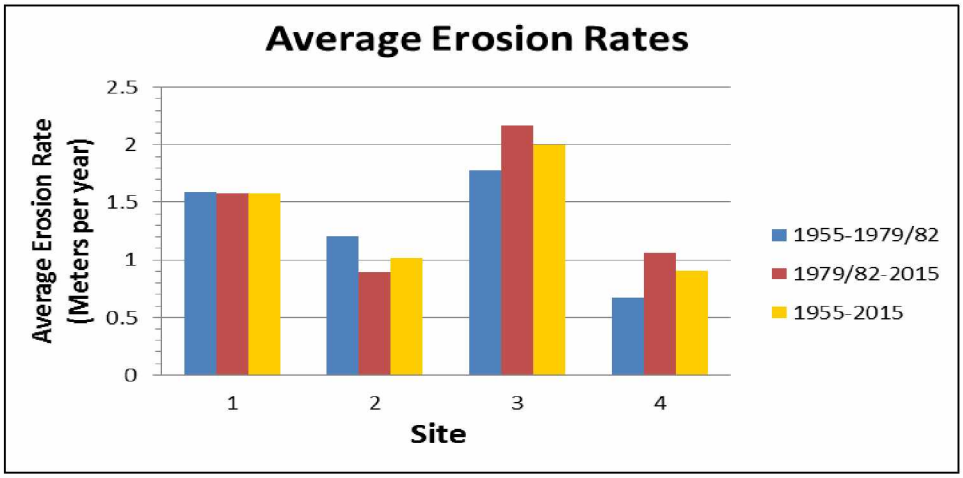

Figure 2.7. Bar graph showing erosional rates at our four study sites.

Site 1: Based on hand-digitized erosion analysis, we found that areas of 25,085 m^2 and 31,959 m^2 were eroded away between 1955 and 1982, and 1982 and 2015, respectively. The total area loss between 1955 and 2015 was 57,044 m^2. With an average elevation of 5.04 m, this equals a total cubic volume loss of 287,502 m^3. Estimating the average bluff retreat (or erosion) along lines perpendicular to the bluff face, we found similar erosion rates of 1.6 m/year for both 1955–1982 and 1982–2015. When estimating cubic volume loss via automated change detection methods, we came out with very low error percentages compared to hand-digitized measurements: the error percentage was 2.05% when comparing the volume estimates for 1955–1982, while the estimate for 1982–2015 was almost perfect, with an error percentage of 0.44%.

Site 2: This was the only site that actually showed a significant reduction in erosion rates between the 1955–1979 and 1979–2015 time periods. Between 1955 and 2015 we calculated an average erosion rate of 1.21 m/year, whereas we only saw 0.89 m/year average erosion between 1979 and 2015. As shown in Table 2.3, we saw very similar erosion volumes for both time periods,

even though 1955–1979 was a 24-year span and 1979–2015 was a 36-year span. This, again, suggests slower rates of erosion over the 1979–2015 time period. As stated previously in this paper, we are unable to determine whether this slowing is indicative of the whole 36-year period, or if there were slower erosion years closer to 1979 that lowered the average for the past 10 to 15 years, which residents report has been a period of increased erosion. Site 2 had the highest error percentages when comparing cubic volume loss estimates; the 9.21% error percentage for 1955–2015 was far higher than other sites, which had percentages as low as 0.44%.

Site 3: This site exhibited both the fastest erosion rates, as well as the largest area of erosion of any site. Average erosion rates increased from 1.78 m/year to 2.17 m/year between the two included time periods. The maximum erosion rate for Site 3 was 3.5 m/year between 1979 and 2015, which was by far the fastest rate of any site over any time period in our study. There was also a large increase in erosion area between the two time periods, from 51,714 m^2 to 97,843 m^2. With an average elevation of 7.51 m, this equates to an estimated cubic volume loss of 1,174,534 m^3 between 1955 and 2015. With such a large square area of erosion at Site 3, it is important to notice the low error percentages for volume estimates: all three digital change detection estimates were lower than 5% error, and as low as 3.13% error for the estimate between 1979 and 2015.

Site 4: Similar to Site 3, Site 4 exhibited increasing erosion rates. From 1979 to 2015, the site had an average erosion rate of 1.06 m/year, which was a 58% increase from the 1955–1979 timespan and shows an average erosion rate of 0.67 m/year. While Site 4 had the slowest erosion rate of all the sites, it did have the largest calculated cubic volume loss, which could be attributed to the large cliff, over 30m high, that occupied the site. Over the 60-year period from 1955 to 2015, Site 4 saw more than 74,000 m^2 of erosion, resulting in 2.5 million m^3 of volume loss. Digital change detection for volume estimations at the site came back with low error percentages ranging from 1.8% to 6.2% error.

2.5.3. Error Analysis

We mapped riverbank erosion at four sites by following two approaches: (1) comparing the location of bluff lines that were hand-digitized using the 1955, 1979/1982, and 2015 images as a base; and (2) using automated change detection between the aforesaid images. As discussed in Section 2.4.1, we coregistered the 1955 and 1979/1982 images to the 2015 WorldView-2 image.

Then, we verified the locational accuracy at 20 sites and observed 2 m or less shift between the images. The pixel sizes of these images ranged from 1.4 m to 2.0 m, so a maximum 2 m of spatial offset represented 1.5 pixels of registration error. In approach (1), we delineated the bluff lines using visual interpretation, and we believe that 0.6 m and 0.3 m differences in pixel sizes had a negligible effect on the accuracy of the bluff line positions, and the estimation of the long-term erosion rate and area. In approach (2), we classified the input images (1979, 1982, and 2015) into three simple land cover classes (water, bare ground, and tundra). The spatial distribution of these classes was such that they were arranged along a sequence of water, bare bluff face, and tundra. Because of this sequential arrangement, the differences in pixel size only affected the pixels along the boundary between two classes. The accuracy of the change detection was, in part, limited by the pixel size of the coarsest resolution input data used. In our study, the 1955 image with 2 m pixel size served as this limiting factor. Given that the lateral bank erosion in the study sites was in the order of tens of meters (at least an order of magnitude higher than the coarsest resolution image), we found the input images appropriate for meeting our change detection needs. In this particular case, the differences in pixel sizes were very small relative to the mapped erosion distances and area, and hence we assumed it had a negligible effect on long-term estimates of erosion rates and area. In the case of approach (1), the only significant source of error in the erosion area mapping was registration error, which propagated into the delineation of the bluff line. The hand-digitized erosion areas at the four sites for all time periods varied from 14,747 m^2 to 149,557 m^2. In order to find out the maximum possible error in erosion area estimation (i.e., the worst-case scenario), we adopted the buffer analysis approach [27]. Hughes et al. [27] used the buffer analysis approach to demonstrate the implications of georectification error when measuring lateral channel movement. We buffered the erosion areas by 2 m and compared the buffered erosion areas with hand-digitized erosion areas. We found that if the 2 m registration error were constant across an entire erosion site, then it could result in 4.3–12.3% error in erosion area mapping. We found the smallest error of 4.3% for the largest erosion polygon, and largest error of 12.3% for the smallest erosion polygon. In this particular case, the registration error only affected the outline of the erosion area, so an erosion polygon with a lower area to perimeter ratio will tend to have higher error. Since the spatial offset between the images varied across the images and was usually less than 2 m, the actual error in calculation of the hand-digitized erosion area was much less than 12.3%. In the case of approach

(2), there are two kinds of error affecting the erosion area estimates: (a) registration error, and (b) land cover classification error. The land cover classification accuracies were 94.4%, 95.6%, and 96.7% for the 1979, 1982, and 2015 images, respectively (Table 2.2). In the last column of Table 3, we reported the difference between the erosion areas estimated using approach (1) and approach (2) as an error percentage (hand-digitized vs. automated), assuming that the hand-digitization of bluff lines is as accurate as possible. The error in mapping and estimation of erosion area by approach (2) varied from 0.44% to 12.8% (Table 2.3). Since we used three simple land cover classes (water, bare land, and tundra) to map erosion in the second method, the majority of the misclassified pixels lay along the boundaries between two classes. Therefore, erosion areas with lower area to perimeter ratios tended to have bigger differences with respect to hand-digitized erosion mapping. For example, in Site 2, which was a near vertical and straight bluff, the erosion area had an area to perimeter ratio of 27 and it also showed the highest error estimate of 9.2% (hand-digitized vs. automated); whereas, Site 1, with an area to perimeter ratio of 43, showed the lowest error estimate of 0.64% (Table 2.3).

2.5.4. Climate Data Results

Figures 2.8 and 2.9 show time series plots of average yearly air temperature, average yearly ground temperature (at 120 cm depth), and average yearly snow depths at USGS weather stations at Fish Creek and Umiat. Air temperature data from the Nuiqsut airport was averaged on a yearly basis and plotted in Figure 2.10. We also examined snow depth data around the river, based on the assumption that higher snow depths, along with warming air temperatures, result in more meltwater during the spring breakup, which has been demonstrated to contribute to greater river erosion [28]. Regression analyses of air and ground temperature, and snow depth data show a statistically significant positive trend in agreement with climate warming and increased snow cover observed in the environment of other Arctic rivers (e.g., Lena River) experiencing increased erosion [1].

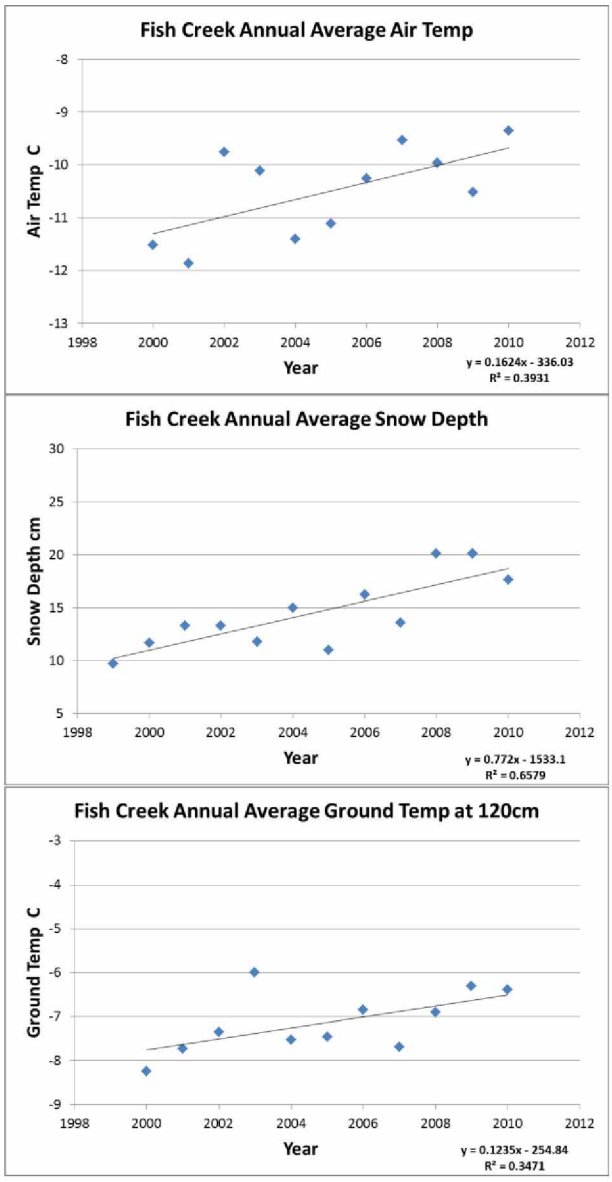

Figure 2.8. USGS climate data averaged annually for Fish Creek, with trend lines overlaid.

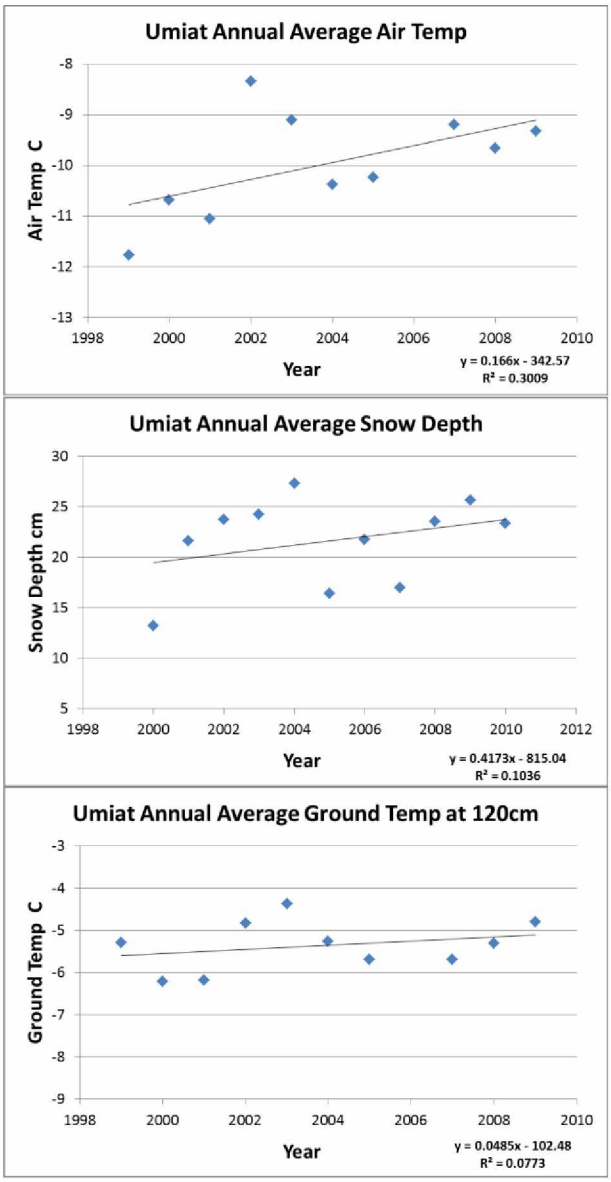

Figure 2.9. USGS climate data averaged annually for Umiat, with trend lines overlaid.

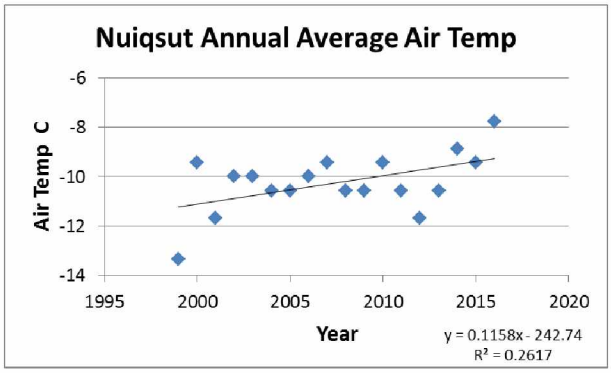

Figure 2.10. Airport air temperature data averaged annually for Nuiqsut, with a trend line overlaid.

As shown in the climate graphs, all sites demonstrated trends of warming temperatures and increasing snow depth. A regression calculation was run for each of the plots at a 95% confidence level. This calculation returned positive results for each of the plots, indicating statistically significant positive trends at each site. Even in our short window of climate data, we see significant warming trends, in the magnitude of multiple degrees. This is on par with Wendler's study on temperature increases in Alaska, which reported an average warming of 2.7 °C across Arctic Alaska from 1979 to 2013, which is a far greater increase than has been observed for any other region or time period in Alaska or for any other climate zones. [6]. This warming has also caused a lengthening of the Arctic melt season at a rate of 4 to 5 days per decade since 1979 [29].

2.6. Discussion

The Colville's high-latitude location lends it unique characteristics. Unlike in most non-Arctic regions, river morphology in the Arctic greatly centers on a few short months of the year when the river is not frozen. The few weeks of breakup and flooding, usually between late May and mid-June, are crucial for river erosion, with nearly 50% of annual discharge into the river occurs during the first three to four weeks of breakup [30]. As a result of this heavy discharge, it is estimated that nearly 75% of annual sediment load is transported during these few weeks of breakup and flooding [12]. Much of this sediment load results from thermal erosion; the process of thawing frozen sediments by turbulent water flow and eroding away what is left by mechanical erosion [31]. Flooding after breakup, caused by the melting of snow in the Colville drainage basin, is one of the largest drivers of erosion for the Colville. The most important impacts of climatic changes in terms of Colville River erosion are thus (a) an increase in snowfall during the winter months, and (b) faster snowmelt during breakup, causing more intense flooding.

According to our estimates of riverbank erosion rates at four sites along the Colville, it is evident that erosion has increased at some sites along the Colville since the 1980s, though the rate of increase in erosion varies spatially, and higher bluff sites tend to have more erosion and land loss (Site 3 and Site 4 in this study). This is due to the fact that the type, timing, and severity of riverbank erosion varies with bank composition and height, snow and ice cover, stage and velocity of discharge, air and water temperature, and wind [8,12]. Most of the banks along the

Colville, upstream of Nuiqsut, range in height from a few meters to 33 m in some large dune areas (e.g., near Site 4), with a general tendency for height to increase upstream. Walker et al. [12] reported a short-term erosion rate of 1.6 m/year (1982–1985) for an erosional bank on Colville made up of Gubik Formation (a Quaternary deposit of unconsolidated sediments). Our estimates of erosion at the Gubik Formation site (Site 1) suggest a long-term erosion rate of 1.6 m/year for both periods (1955–1982) and (1982–2015), which means that this site has been eroding consistently at 1.6 m/year rate since 1955.

Much higher rates of riverbank erosion have been reported from other Arctic rivers. Costard et al. [8] reported exceptionally high erosion rates of up to 40 m/year along the Lena River banks in specific areas (e.g., concave river banks and heads of islands). Based on a laboratory simulation experiment, they concluded that the exceptional erosion rates were due to a combination of high water temperature and mechanical erosion, in association with the particular geometry of the channel. Are [32] reported average bank retreats of 19–24 m/year on the Lena River during 1953–1961. However, in the Olenek channel of the Lena River delta, the bank retreated at an average rate of 1.7 m/year, which is comparable to the erosion rates we found along the Colville.

Kanevskiy et al. [9] investigated the riverbank retreat at three active yedoma bluff sites along the Itkillik River, a tributary of the Colville River. They reported the highest long-term rates of riverbank erosion ever observed in permafrost regions of North America. For one of their study sites, they reported an average retreat rate for a 680-m-long bluff as 11 m/year (1995–2010). They also found that lower bluffs (height of <4.5 m) tended to have much lower retreat rates. Contrary to this finding, we observed the lowest erosion rate at the tallest bluff site (Site 4: average height of 33 m with an erosion rate of 0.9 m/year during 1955–2015), and the highest erosion rate of 2 m/year (1955–2015) at Site 3, which had an average elevation of 7.5 m.

Stettner et al. [10] estimated cliff top erosion of a permafrost riverbank in the central Lena River Delta. They reported a short-term (2013–2015) mean annual net erosion of 4.1–6.9 m/year, which is close to the reported rates of riverbank cliff-top erosion at the Yana and Indigirka river delta sites [11]. They concluded that the mean annual net erosion at their study site significantly differed from one year to another, and analysis of the role of climate variables on erosion suggested a contingent sensitivity of erosion to temperature and precipitation. Air temperature has a strong influence on erosion, but when temperatures are at or below average precipitation

appears to be an important factor. In situations where the cliff top is decoupled from the thermo-erosional processes, its erosion likely results from climate forcing, and depends on bank composition and ground ice content.

Along most parts of the Colville River bank (particularly banks with lower height), development of thermoerosional niches, followed by block collapse, is the dominant process of bank retreat; whereas, along the higher banks, such as Site 4, where the upper part of the bluff is decoupled from the thermo-erosional processes, thermal denudation is the dominant process of bank retreat. Our estimates of riverbank erosion at four sites on the Colville are very similar to the rates reported by Walker et al. [12], and contrast greatly with the erosion rates reported for Siberian rivers [8,10,32], and the Itkilik River [9]. The block collapse that often follows the development of thermoerosional niches accounts for an almost instantaneous retreat that can be as much as 12 m [12]; however, long-term rates, even in susceptible cut banks, rarely exceed 3 m.

The majority of erosion studies analyze erosion in terms of short-term or long-term rates and do not include changes in erosion area or land loss volume [8,10–12]. For example, Shur et al. [11] studied river shoreline erosion at 14 sites along the Yana and Indigirka Rivers in North Yakutia and analyzed only average erosion rates. Walker et al. [12] studied riverbank erosion at six sites in the Colville River Delta; however, they reported total land volume loss at only one site. Kanevskiy et al. [9] estimated land volume loss at three bluff sites along the Itkilik River for the short period of 2007–2011 but did not show how the land loss compared with land loss for an earlier period. Stettner et al. [10] estimated only the erosion rate to study riverbank erosion in the central Lena Delta.

The average erosion rate (i.e., erosion distance divided by timespan in year) does not necessarily provide a complete picture of the amount and severity of bank erosion. Hence, to get a better understanding of the riverbank erosion process on the Colville, we not only estimated long-term erosion rates, but also changes in erosion area and volume of land loss. At Site 1 (Gubik Formation), the average erosion rate turned out to be 1.6 m/year for both the 1955–1982 and 1982–2015 periods; however, the estimated erosion area increased from 25,085 m^2 during 1955–1982 to 31,959 m^2 during 1982–2015. Therefore, in terms of the average erosion rate, the rate of erosion appeared to be consistent at this site, but in reality, erosion had a disproportionally greater effect during the 1982–2015 period. Similarly, at Site 3, the difference in the erosion rate for the period 1955–1979 and 1979–2015 was 1.8 and 2.2 m/year, respectively, but the difference in

the erosion area almost doubled from 51,714 m^2 to 97,843 m^2. At Site 4, the difference in the erosion rate for the period 1955–1979 and 1979–2015 was 0.7 and 1.0 m/year, respectively, but the difference in the erosion area more than doubled from 23,884 m^2 to 50,352 m^2. When we compared the average erosion rate at Site 1 (1.6 m/year) to Site 4 (1.0 m/year), we saw that Site 1 had a much higher erosion rate. However, Site 4 had the tallest banks (average bank height of 33 m) and the volume of land loss was 1,689,813 m^3 for the period 1979–2015, which was 10 times more land volume loss than at Site 1 (average bank height of 5 m) for the same period.

Erosion and deposition also alter the connectivity of secondary channels and lakes to the main channel of the Colville, which impacts fish habitat [33], as well as accessibility of traditional subsistence and historical sites to the residents of Nuiqsut. When the river erodes faster than the channel can carry sediment to the sea, the sediment deposits in the river system itself and can close up smaller channels or create hazardous shallow sites in the main channel. Popular lakes can become inaccessible or drain due to bank erosion [34]. During our fieldwork, we noted an example of this at Site 3, where a large lake had drained in the early summer of 2017, as described by local residents who had previously used the lake as a fishing site (Figure 2.11). These changes impact the subsistence lifestyle of Nuiqsut residents, who rely heavily on

Figure 2.11. Lake near Site 3 that has drained due to bank erosion.

traditional knowledge passed down from generation to generation. Elders possess a wealth of knowledge about the Colville, but in recent times the river has become so dynamic that it is hard to keep up with the changes, posing a real threat to subsistence practices. Updated knowledge of the characteristics and rate of change to the Colville would be valuable information for making management decisions about river access for the community.

The accuracy of measuring erosion by hand-digitization versus automated change detection methods is significant for large-scale Arctic river monitoring. In the case of measuring erosion by hand-digitization, the major source of error is registration error, and in the case of the automated change detection method, the major sources of error are registration error and classification error. In both cases, these errors tend to have the greatest effect along the outline of an erosion area or along the boundary between the land cover classes. Therefore, erosion areas with lower area to perimeter ratios tend to have higher error. By minimizing registration error and improving land cover classification accuracy, the overall error in erosion area mapping can be minimized.

We determined that, for the study of a small number of sites such as those in our study, hand-digitized measurements were the most accurate method for estimating erosional rates and areas. However, if the goal of a study is to monitor yearly river erosion on a large scale, our results indicate that automated change detection methods can produce reasonable estimates. This serves to validate a straightforward and rapid process for monitoring river erosion that can be performed by someone with even limited GIS and image processing skills.

Our use of DEM trajectories to estimate paleo cliff elevations may be unique to the Arctic. We are confident in our estimates due to the geomorphology of our study area, a relatively flat region with little change in topography.

2.7. Conclusions

Analysis of high-resolution data indicates that bank erosion on the Colville River seems to have increased during the past 36 years, from 1979/1982 to 2015, when compared to erosion from 1955 to 2015. Of four erosion sites analyzed, two showed significant increases in yearly erosional rates from 1.8 m/year to 2.2 m/year and from 0.7 m/year to 1.0 m/year. One site showed similar erosion rates of 1.6 m/year between the two time periods, and a fourth site showed a decrease in erosion rates from 1.2 m/year to 0.8 m/year. However, the average erosion

rate (i.e., erosion distance divided by timespan) did not necessarily provide a complete and accurate picture of the extent and severity of bank erosion. Hence, to get an accurate understanding of the riverbank erosion process of the Colville, we not only estimated the long-term erosion rates, but also changes in erosion area and the volume of land loss. At Site 3, the average erosion rate for the period 1955–1979 and 1979–2015 was 1.8 and. 2.2 m/year, respectively, but the difference in the erosion area was almost double, from 51,714 m^2 to 97,843 m^2. At Site 4, the average erosion rate for the period 1955–1979 and 1979–2015 was 0.7 and 1.0 m/year, respectively, but the difference in the erosion area was more than double, from 23,884 m^2 to 50,352 m^2. When we compared the average erosion rate at Site 1 (1.6 m/year) to Site 4 (1.0 m/year), we saw that Site 1 had a much higher erosion rate. However, Site 4 had the tallest banks (average bank height of 33 m) and the volume of land loss was 1,689,813 m^3 for the period 1979–2015, which was ten times more than the volume of land loss at Site 1 (average bank height of 5 m) for the same period.

The novelty of this research is in extending the estimates from two-dimensional surface erosion rates (as reported by most studies) to three-dimensional volumes (i.e., the amount of material eroded). Whereas there is a wealth of literature available on the former, there is very little published on the latter. As per our knowledge, this is the first paper that demonstrates that for an Arctic river, studies on riverbank erosion that use only erosion rate can be inaccurate and grossly conservative. This study validates the significance of mapping erosion areas and estimating land loss volumes to gain an accurate understanding of the amount and severity of riverbank erosion, as in certain areas the volume of land loss can be disproportionately higher than what average erosion rates may suggest. Hence, this study presents not only an improved understanding of the extent and severity of riverbank erosion along parts of the Colville than any previous study, but also valuation of land loss from typical eroding banks using publicly available DEM.

Based on the erosion study results and climate data, it can be safely inferred that climate warming plays a role in erosion on the Colville. These findings are consistent with a study on increased erosion due to climate change on the Lena River in Central Siberia, an Arctic fluvial system similar to the Colville [1]. Air and ground temperature warming trends on the North Slope are likely the catalyst for increased erosion rates through the thawing of permafrost along river bluffs causing massive block failure. Warmer temperatures also mean longer ice-free

seasons, which results in a longer period in which the river can erode. Trends of higher snow depths contribute to more meltwater during the spring breakup, which is the main period of erosion for Arctic rivers. If these climate trends continue, it can be inferred that erosion along the Colville will continue to increase, resulting in more problems for the residents of Nuiqsut, who rely on the river to travel to subsistence and historical family sites. Additionally, important village infrastructure, such as a water tank and power plant, is located within 90 m from an eroding bluff (near Site 1). If the rate of erosion intensifies, this will have major economic implications for the village of Nuiqsut.

This study suggests that high-resolution imagery can be effectively used to monitor bluff line erosion along Arctic rivers. This type of monitoring can enhance our understanding of hydro-geomorphological processes along Arctic rivers and provide information for estimates of future change. We have also demonstrated that estimating erosion via automated change detection based on simple classification methods can be as effective as digitizing by hand. This is important for monitoring large study areas or making multiple change observations in areas where hand-digitization is not feasible. We have also successfully used a current DEM to calculate the cubic volume of past erosion, and demonstrated the efficacy of this simple method for paleo topography estimates for relatively flat Arctic regions. This method can be used in certain situations when land topography changes are minimal and no other source of data is available to gauge the height of eroded features.

Though this study returned solid results, it was hampered by several limitations, primarily the lack of high-resolution cloud-free imagery for the 2000–2013 time period. Such imagery would have been ideal in order to examine more recent erosion trends, as local knowledge from Nuiqsut suggests that erosion increases have not been linear since 1979, but almost exponential, with the greatest erosion happening in the past 10 to 15 years. We speculate that climate warming is also warming water temperatures, which can expedite the processes of thermal erosion along riverbanks. Future erosion studies could potentially incorporate more variables, such as water temperature.

This study delivered significant results, crucial to the community of Nuiqsut, while simultaneously adding novel techniques to the remote sensing of river erosion literature. We expect that the regular availability of high-resolution summer imagery in the future will enable continued monitoring of river erosion using the techniques presented in this paper.

Acknowledgments: This work was supported by an Alaska NSF EPSCoR award #OIA-1208927 and the state of Alaska, as well as the Alaska Space Grant and the UAF Global Change Student Research Grant. The authors would like to thank Tom Moran for editorial assistance, Matthew Whitley for help with preparation of the GIS data, and Todd Brinkman for his insight on erosion along the Colville.

Author Contributions: C.P. and S.P. conceived and designed the study; C.P. and S.P. performed the fieldwork; C.P. processed the data; C.P., S.P., and A.P. analyzed the data; C.P. led the writing; S.P. and A.P. contributed to the writing.

Conflicts of Interest: The authors declare no conflict of interest.

References

1. Costard, F.; Gautier, E.; Brunstein, D.; Hammadi, J.; Fedorov, A.; Yang, D.; Dupeyrat, L. Impact of the global warming on the fluvial thermal erosion over the Lena River in Central Siberia. *Geophys. Res. Lett.* **2007**, *34*, L14501, doi:10.1029/2007GL030212.
2. Tananaev, N.I. Hydrological and geocryological controls on fluvial activity of rivers in cold environments. In Cold and Mountain Region Hydrological Systems under Climate Change: Towards Improved Projections, Proceedings of the H02, IAHS-IAPSO-IASPEI Assembly, Gothenburg, Sweden, 22–26 July 2013; IAHS Publ.: Gothenburg, Sweden, 2013 pp. 161–167.
3. Walker, H. *Some Aspects of Erosion and Sedimentation in an Arctic Delta during Breakup*; Coastal Studies Institute, Louisiana State University: Baton Rouge, LA, USA, 1970; pp. 209–219.
4. BurnSilver, S.; Magdanz, J.; Stotts, R.; Berman, M.; Kofinas, G. Are mixed economies persistent or transitional? Evidence using social networks from Arctic Alaska. *Am. Anthropol.* **2016**, *118*, 121–129, doi:10.1111/aman.12447.
5. Schmidt, J.; Kofinas, G.; Brinkman, T. *Local Knowledge and Science: Observations of Landscape Change in the Nuiqsut Homelands*; University of Alaska Anchorage and Fairbanks: Anchorage, AK, USA. Available online: http://www.alaska.edu/epscor/ (accessed on 18 February 2018)
6. Wendler, G.; Moore, B.; Galloway, K. Strong temperature increase and shrinking sea ice in Arctic Alaska. *Open Atmos. Sci. J.* **2014**, *8*, 7–15.

7. Floyd, A.; Prakash, A.; Meyer, F.; Gens, R.; Liljedahl, A. Applicability of Synthetic Aperture Radar to investigate river ice breakup on the Kuparuk River, Northern Alaska. *Arctic* **2014**, *67*, 462–471, doi:10.14430/arctic4426.
8. Costard, F.; Dupeyrat, L.; Gautier, E.; Carey-Gailhardis, E. Fluvial thermal erosion investigations along a rapidly eroding river bank application to the Lena River (central Siberia). *Earth Surf. Process. Landf.* **2003**, *28*, 1349–1359, doi:10.1002/esp.592.
9. Kanevskiy, M.; Shur, Y.; Strauss, J.; Jorgenson, T.; Fortier, D.; Stephani, E.; Vasiliev, A. Patterns and rates of riverbank erosion involving ice-rich permafrost (yedoma) in northern Alaska. *Geomorphology* **2016**, *253*, 370–384, doi:10.1016/j.geomorph.2015.10.023.
10. Stettner, S.; Beamish, A.L.; Bartsch, A.; Heim, B.; Grosse, G.; Roth, A.; Lantuit, H. Monitoring inter-and intra-seasonal dynamics of rapidly degrading ice-rich permafrost riverbanks in the Lena Delta with TerraSAR-X time series. *Remote Sens.* **2017**, *10*, 51, doi:10.3390/rs10010051.
11. Shur, Y.; Vasiliev, A.; Kanevsky, M.; Maximov, V.; Pokrovsky, S.; Zaikanov, V. Shore Erosion in Russian Arctic. In Cold Regions Engineering: Cold Regions Impacts on Transportation and Infrastructure, Proceedings of the 11th International Conference on Cold Regions Engineering 2002, Anchorage, AK, USA, 20–22 May 2002; American Society of Civil Engineers: Anchorage, USA, 2002; pp. 736–747.
12. Walker, J.; Arnborg, L.; Peippo, J. Riverbank erosion in the Colville delta, Alaska. *Phys. Geogr.* **1987**, 61–70, doi:10.2307/521367.
13. Alaska EPSCoR Data Portal. Available online: http://epscor.alaska.edu/search (accessed on 18 January 2018).
14. Digital Globe Inc. Available online: https://www.digitalglobe.com (accessed on 18 January 2018).
15. Polar Geospatial Center at the University of Minnesota. Available online: https://www.pgc.umn.edu (accessed on 18 January 2018).
16. USGS Climate and Active-Layer Data. Available online: https://pubs.usgs.gov/ds/812/introduction.html (accessed on 18 January 2018).
17. Weather Underground. Available online: https://www.wunderground.com/weather/us/ak/nuiqsut (accessed on 18 January 2018).

18. Winterbottom, S.J.; Gilvear, D.J. A GIS-based approach to mapping probabilities of river bank erosion: Regulated River Tummel, Scotland. *River Res. Appl.* **2000**, *16*, 127–140, doi:10.1002/(SICI)1099-1646(200003/04)16:2<127::AID-RRR573>3.0.CO;2-Q.
19. Lawler, D.M. The measurement of river bank erosion and lateral channel change: A review. *Earth Surf. Process. Landf.* **1993**, *18*, 777–821, doi:10.1002/esp.3290180905.
20. Swain, P.; Davis, S. *Remote Sensing: A Quantitative Approach*; McGraw-Hill Book Co.: New York City, NY, USA, 1978; 396 p.
21. Richards, J. *Remote Sensing Digital Image Analysis*; Springer: Berlin/Heidelberg, Germany, 1986; 292 p.
22. Bolstad, P.; Lillesand, T. Rapid maximum likelihood classification. *Photogramm. Eng. Remote Sens.* **1991**, *57*, 67–74.
23. Otukei, J.; Blaschke, T. Land cover change assessment using decision trees, support vector machines and maximum likelihood classification algorithms. *Int. J. Appl. Earth Obs. Geoinf.* **2010**, *12*, S27–S31.
24. Panda, S.K.W.; Whitley, M. Sixty-five Years of Colville River Dynamics and its Impact on Present River Navigability near Nuiqsut, North Slope of Alaska. In Proceedings of the 14th International Circumpolar Remote Sensing Symposium, Homer, AK, USA, 12–16 September 2016. Available online: https://alaska.usgs.gov/science/geography/CRSS2016/posters_and_talks/Whitley_ICRSS_Poster_compressed.pdf (accessed on 23 February 2018).
25. Congalton, R.G. A review of assessing the accuracy of classifications of remotely sensed data. *Remote Sens. Environ.* **1991**, *37*, 35–46, doi:10.1016/0034-4257(91)90048-B.
26. Mars, J.; Houseknecht, D. Quantitative remote sensing study indicates doubling of coastal erosion rate in past 50 yr along a segment of the Arctic coast of Alaska. *Geology* **2007**, *35*, 583–586, doi:10.1130/G23672A.1.
27. Hughes, M.L.; McDowell, P.F.; Marcus, W.A. Accuracy assessment of georectified aerial photographs: Implications for measuring lateral channel movement in a GIS. *Geomorphology* **2006**, *74*, 1–16, doi:10.1016/j.geomorph.2005.07.001.
28. Walker, H.J.; McCloy, J.M. *Morphologic Change in Two Arctic Deltas*; Arctic Institute of North America: Washington, DC, USA, 1969.

29. Stroeve, J.; Markus, T.; Boisvert, L.; Miller, J.; Barrett, A. Changes in Arctic melt season and implications for sea ice loss. *Geophys. Res. Lett.* **2014**, *41*, 1216–1225, doi:10.1002/2013GL058951.
30. Arnborg, L.; Walker, H.J.; Peippo, J. Water discharge in the Colville River. *Phys. Geogr.* **1966**, *48*, 195–210, doi:10.2307/520502.
31. Gatto, L.W. *Soil Freeze-Thaw Effects on Bank Erodibility and Stability*; Accession Number: ADA301818; Cold Regions Research and Engineering Lab: Hanover, NH, USA, 1995. Available online: http://www.dtic.mil/dtic/tr/fulltext/u2/a301818.pdf (accessed on 18 January 2018).
32. Are, F. Thermal Abrasion of Coasts. In Proceedings of the Fourth International Conference on Permafrost, Washington, DC, USA, 17–22 July 1983; University of Alaska Fairbanks: Fairbanks, AK, USA, 1983; pp. 24–28.
33. Brubaker, M.; Bell, J.; Dingman, H.; Itta, M.; Kasak, K. *Climate Change in Nuiqsut, Alaska, Strategies for Community Health*; Publication of the Center for Climate and Health, Alaska Native Tribal Health Consortium: Anchorage, AK, USA, 2014. Available online: http://www.north-slope.org/assets/images/uploads/ANTHC_Nuiqsut_7-31-14_web_FINAL.pdf (accessed on 18 January 2018).
34. Jones, B.M.; Arp, C.D. Observing a catastrophic thermokarst lake drainage in northern Alaska. *Permafr. Periglac. Process.* **2015**, *26*, 119–128, doi:10.1002/ppp.1842.

Chapter 3

[2]Remote Monitoring of Shallow Water Sites to Inform Boat Navigation on the Colville River, Alaska: A Feasibility Study

Abstract

The Colville is the longest river (~600 km) in Arctic Alaska. Nuiqsut, an established Alaska Native community of ~400 people relies heavily on the Colville for subsistence needs, however, changing river dynamics caused by accelerated bank erosion, river siltation, low water, and shifting and drying channels are making boat travel increasingly difficult and dangerous. Recently, local residents reported unexpected shallow water sections on the Colville limiting their access to subsistence food sources, and expressed the need for maps that aid river navigation. These concerns shaped the goals of this study: 1) use optical satellite images for mapping river bathymetry and generate GIS map products that show potential shallow water sections (<2m) and 2) assess the feasibility of future monitoring based off our methods that rely on extracting water depth values from publicly available optical remote sensing images.

We used summer 2017 scenes from three optical sensors (PlanetScope 3m, Sentinel 2 10m, and Landsat 30m) along with field measurements to map shallow water bathymetry along a 45 km stretch of the Colville. We found a strong correlation (R2=0.89) between field-measured water depths and image-derived reflectance quantity (natural log ratio of green over red bands). We analyzed suitable bathymetry conditions and expect several days (≈16) during the ice-free season to facilitate reliable bathymetry mapping. We also discuss a relative depth mapping technique which is useful for boat navigation in the absence of ground truth measurements. We deliberately employed simple and robust empirical techniques that could serve as a basis for a fully developed river monitoring project in the near future led by local community residents. An implementation of our methods by the community, in order to develop a river depth monitoring

[2] Article submitted as Payne C, Panda S, Prakash A, Brinkman T. Remote Monitoring of Shallow Water Sites to Inform Boat Navigation on the Colville River, Alaska: A Feasibility Study. Environmental Research Letters.

program, would be an important step forward for the advancement of the community-based science and the co-production of knowledge.

3.1 Introduction

Traditionally, studies of river bathymetry contribute to the understanding of sediment transportation (Dankers 2002), catchment-scale hydrology (Bryant and Gilvear 1999), and flood modeling (Horritt et al. 2002, Lotsari et al. 2010). Our study uses river bathymetry to address an emerging issue of boat navigation in Arctic Alaska, a region with virtually no roads, where residents use the rivers to travel for their subsistence hunting needs as well as to reach traditional camp sites (Braund et al. 2017). Recently residents of Nuiqsut have expressed concern that climate-related changes have created shallow water conditions and unpredictable changes to the Colville River channels, challenging boat access to subsistence areas (Moerlein and Carothers 2012, Brubaker et al. 2014, Brinkman et al. 2016, ANTHC 2016). Shallow water spots on the river create hazardous conditions for traditional propeller boat travel and limit access to channels that have been used in the past. These conditions can be costly (e.g. boat repairs), present safety issues, and restrict harvest opportunities (White et al. 2007). With a goal to address these concerns, we engaged with the local residents, designed a remote sensing based scientific study, and delivered results in a format that optimizes utility for the community following the best practices for co-production of knowledge and making science locally relevant (Armitage et al. 2011, Meadow et al. 2015).

Remote sensing based bathymetry mapping can be classified into two broad categories: a) non-imaging (Charlton et al. 2003, Hilldale and Raff 2008, Legleiter 2012, Kinzel et al. 2013) (e.g. using high cost LiDAR data), and b) imaging methods (e.g. using low cost optical satellite imagery) (Gao 2009, Legleiter et al. 2009, Legleiter 2013) that can further include analytical and empirical approaches. The empirical approaches, originally developed for ocean bathymetry (Polcyn et al. 1970, Lyzenga 1978, 1981, Clark et al. 1987) and now adapted for stream and river use (Winterbottom and Gilvear 1997, Bryant and Gilvear 1999, Marcus et al. 2003, Legleiter et al. 2004, 2009, Flener et al. 2012), involve fewer parameters and are relatively simple to use (Gao 2009, Legleiter 2013). However, the use of passive remote sensing for mapping water depth in fluvial environments remains a challenge (Flener et al. 2012, Panda and Whitley 2017, Legleiter et al. 2018). All previous research but one that used imaging methods for bathymetry

focused on small non-Arctic rivers or streams (e.g. Winterbottom and Gilvear 1997, Legleiter et al. 2004, 2009). The only study on an Arctic river (Flener et al. 2012) evaluated and compared the usability of an empirical model against two theoretical hydraulically assisted models for calculating bathymetry along a very small (2.7 km) stretch of the Tana River in Finland.

This study is unique as it uses imaging method and empirical approaches to map bathymetry on a large Arctic river (often 600 m wide) for a novel application of river navigation. It also assesses the feasibility of continued monitoring of shallow water conditions on the Colville using simple and robust methods that can be repeated by community members (e.g. a staff member of the Native Village Office or North Slope Science Initiative). The specific objectives of the study are 1) to use optical satellite images for mapping river bathymetry to produce GIS map products showing potential shallow water sections (<2m) and poor channel connections to aid river navigation, and 2) to assess the feasibility of future monitoring based off our methods and publicly available imagery. We also identified the criteria essential to map bathymetry from optical remote sensing images and discussed the likelihood of meeting those criteria in the future for the purpose of continued monitoring which helps determine the overall feasibility of the study.

3.2 Study Area

The Colville is the longest river in the Alaskan North Slope with a course of 600 km. It is also the largest river basin (53,000 km^2) north of the Brooks Range in Arctic Alaska. The river drains the north side of the Brooks Range and winds its way into a 550 km^2 delta 250 km east of the community of Utqiagvik (formerly Barrow) before emptying into the Beaufort Sea (Arnborg et al. 1966) (Figure 3.1). For this study we chose a 45 km stretch of the Colville (upstream from the village of Nuiqsut past Ocean Point) heavily used by Nuiqsut residents between early June and September.

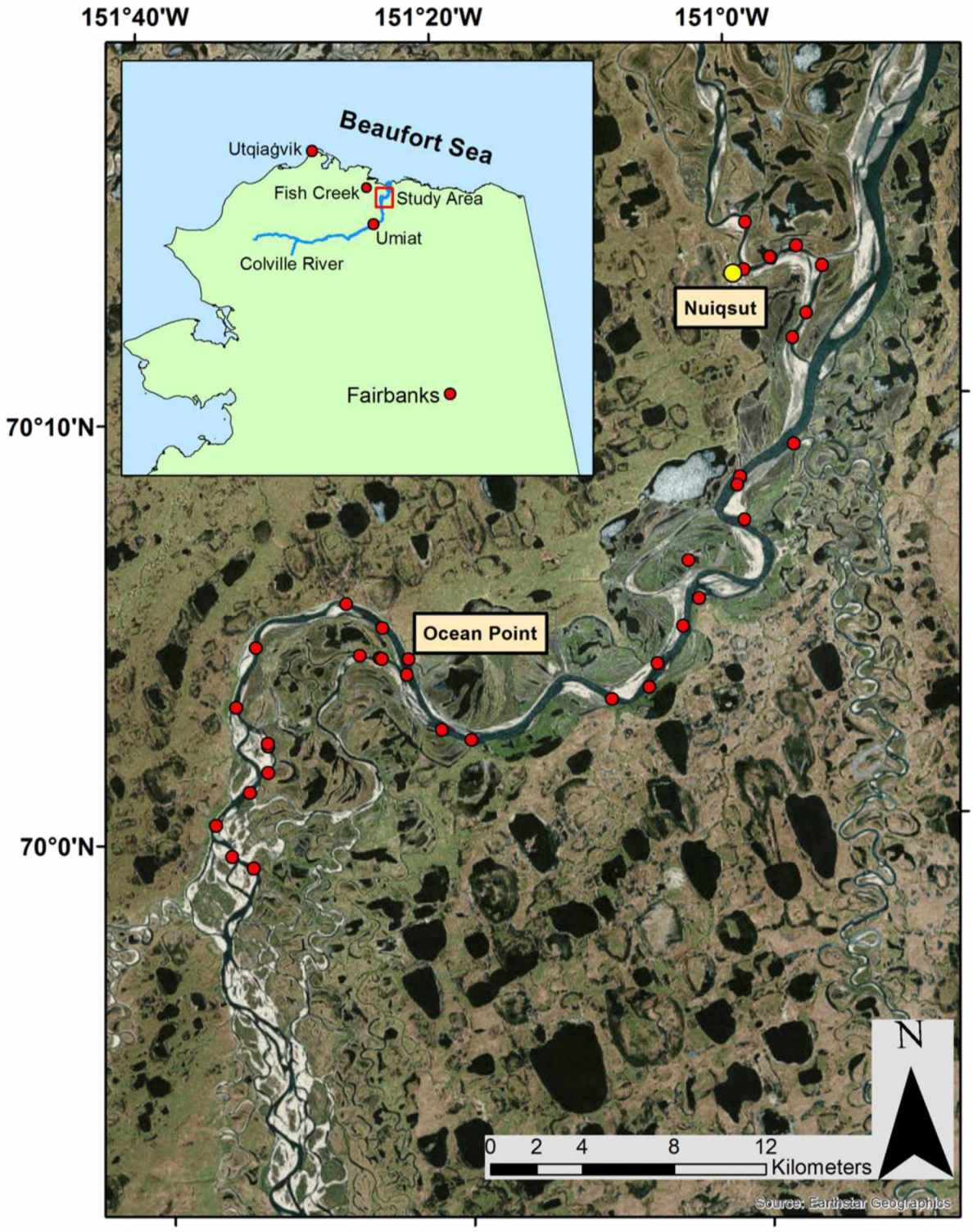

Figure 3.1. Study area map. The red box in the inset figure shows the location of the study area. In the main figure red dots show the location of field sampling sites on the Colville.

3.3 Data

We used optical images from three different satellites (PlanetScope, Sentinel 2, and Landsat 8) for the period June 15 – September 30, 2017, the main ice-free season for the Colville as well as the most heavily trafficked period for boat travel by Nuiqsut residents. We also used in situ measurements of water depth and turbidity, and climate data from local weather stations (Table 3.1; more details in Appendix).

Table 3.1. Data used for our study

Data Type	Details	Time Period	Data Sources
PlanetScope 4 band optical imagery	3m spatial resolution Blue 455 – 515 nm Green 500 – 590 nm Red 590 – 670 nm NIR 780 – 860 nm	Summer 2017	Planet Labs
Sentinel 2 imagery	10 m spatial resolution Blue 447 – 545 nm Green 537 – 583 nm Red 645 – 683 nm NIR 762 – 907 nm	Summer 2017	European Space Agency
Landsat 8 imagery	30 m spatial resolution Blue 452 – 512 nm Green 533 – 590 nm Red 636 – 673 nm NIR 851 – 879 nm	Summer 2016 & 2017	United States Geological Survey
Nuiqsut Climate Data	Cloud cover, Rainfall	2010 - 2017	Weather Underground
Field Data	Water depth, Turbidity	July 31- Aug. 1 2017	Collected by authors
Traditional Ecological Knowledge	Firsthand knowledge from semi-structured conversations	2017	Collected by authors

3.4 Methods

Using the summer 2017 remote sensing and field data, we first carried out a proof of concept study to establish bathymetric mapping methods and to assess if the bathymetry map products were practical and useful in field settings. We then identified and analyzed the factors

that govern reliable bathymetry monitoring: expected future image availability, cloud cover, water turbidity levels, use of different optical sensors, and limited ground truth data.

3.4.1 Community Involvement

From the beginning this study was designed with the community need and involvement in mind (IRB# 391916). Our goal was to follow a coproduction of knowledge approach (Armitage et al. 2011, Meadow et al. 2015) that used community-based participatory research (Johnson et al. 2015) to engage the Nuiqsut residents in research that addressed both community priorities and scientific questions related to the impacts of rapid environmental change (Gearheard et al. 2010, Payne et al. 2018). We consulted with local Tribal organizations on guidelines and ethical principles to co-produce knowledge within the community. The Colville is the main subsistence travel corridor for Nuiqsut residents and provides the community with resources that are nutritionally and culturally important (Brubaker et al. 2014). The community identified the need to research river channel change and challenges to boat navigability, especially shallow areas in the main channel of the river and frequent unpredictable changes in the navigable part of the river.

Locals were hired to transport researchers and to share traditional knowledge on the importance of the river and how recent changes are impacting traditional harvest practices. Interactions with the community also defined our field sampling area, a stretch of the river used by the majority of local residents for subsistence, and key trouble spots for navigation. The local assistance facilitated safe travel and provided important contextual information that would help with data interpretation. Off the boat, our local collaborators provided us with valuable connections in the community that facilitated semi-structured conversations with more residents, and advanced our understanding of how the issue of shallowing water has been affecting people from multiple perspectives.

Adhering to our co-production approach, we sought to create a product useful to the community but also replicable by the community. The community has expressed interest to continue this work, which may lead to development of a Rapid Assessment Tool (RAT) that would enable the community to assess the state of the river channel between Umiat and the Arctic Ocean in near real time (<1 week). A visual tool like this would be beneficial for the

community of Nuiqsut and applicable to rural communities in other areas reliant on safe and dependable river travel (Herman-Mercer et al. 2011, Wilson et al. 2015, Johnson et al. 2016).

3.4.2 Turbidity Assessment

Turbidity is an optical property of the water body – a measure of the amount of light scattered and absorbed by particles in the water column (Michaud 1991). Higher turbidity levels mean more sediment in the water that in turn creates high levels of light attenuation throughout the water column (Davies-Colley and Smith 2001). This reduces visual range in water and makes it tough to map river bathymetry which relies on reflectance from the river bottom (Legleiter et al. 2009). A clear water column with low turbidity values interferes minimally with the river bottom reflectance that makes bathymetry mapping possible. Therefore, determining a turbidity level threshold for reliable mapping of bathymetry from optical images is an important part of assessing the feasibility of future bathymetry mapping on the Colville.

We measured NTU values on the river for two dates, July 31st 2017 and August 5th 2016 (Whitley et al. 2016, Panda and Whitley 2017) and had cloud free scenes close to the dates of these field measurements. For both dates the NTU values were minimal and within a small range (July 31st, 2017: 15.4 ± 11.3 NTU; August 5th, 2016: 14.5 ± 4.3 NTU). See Figure A1 (Appendix).

3.4.3 Normalized Difference Water Index

The Normalized Difference Water Index (NDWI) is a good indicator of presence of open water (McFeeters 1996):

$$NDWI = (Green - NIR) / (Green + NIR) \quad (1)$$

Water features have high reflectance in the green bands and very low reflectance in the NIR bands. Terrestrial vegetation and dry soils, on the other hand, reflect highly in NIR. In an NDWI layer, water features have positive values while soil and terrestrial vegetation features have zero or negative values (McFeeters 1996). NDWI is also shown to have a close correlation to water turbidity levels (McFeeters 1996, and Xu 2006). In order to assess the water turbidity levels from the images we compared the known NTU values from the two fieldwork dates with

the Normalized Difference Water Index (NDWI) generated from the images near the dates of field turbidity measurements.

We used a calculated NDWI raster to identify river water pixels and to create a river water mask (Figure 3.2) that was used to extract river water pixels for NDWI-turbidity comparisons as well as bathymetric calculations. We analyzed average river water NDWI values (over the whole study area) from 9 cloud-free scenes including the two with ground truth NTU values to identify the average NDWI threshold that can be used to select images that have clear enough water to map reliable bathymetry (Figure A2).

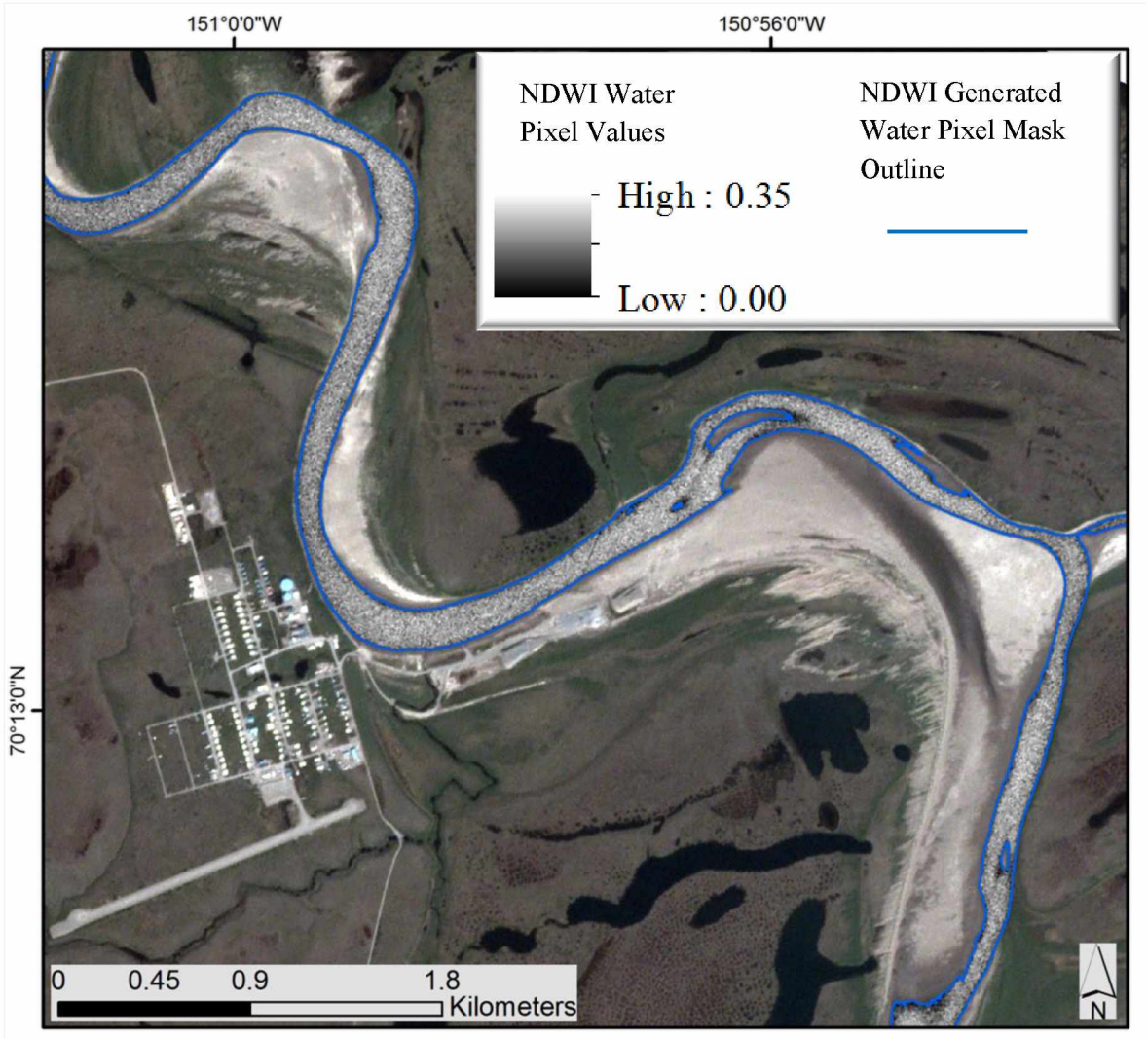

Figure 3.2. NDWI pixels from July 14th 2017 image extracted using the water pixel mask (outlined in blue) and overlaid on July 14th 2017 RGB PlanetScope image.

3.4.4 Bathymetry Mapping

For bathymetry mapping we chose to use an empirical approach (Legleiter et al. 2004, 2009) that fosters replication by a community member. Empirical remote sensing bathymetry methods rely on the concept of relating river reflectance over a water pixel to water depth. Over deeper water more reflected signal from the bottom gets attenuated by the water column above and therefore would give smaller reflectance values than over shallow water. We used a ratio based empirical method (Equation 2) that works best for relatively shallow water (< 2 m) to map river bathymetry (Lubin et al. 2001, Stumpf et al. 2003, Legleiter et al. 2009, Legleiter 2013, Whitley et al. 2016).

$$x = ln(Band\ 1 / Band\ 2) \quad (2)$$

This method uses the natural log ratio of two bands that can be regressed against known depth points. The advantage of the ratio method is its ability to be less affected by factors such as spatially variable water surface conditions, turbidity, and most importantly bottom substrate type, which can be a large problem for remote sensing based bathymetry (Legleiter et al. 2004). Legleiter et al. (2009) expanded upon the ratio based method by introducing Optimal Band Ratio Analysis (OBRA). This technique examines each possible band combination in the above formula to see which output correlates best to the known data points in terms of the highest R^2 value on a regression plot. For this study we chose to use OBRA (Figure A3).

There is a PlanetScope scene for the day we were in the field but around 90% of the scene is cloud covered. The small portion of the scene that is cloud-free overlapped with two measurements we took on the river, which helped us correct for changes in water depth between the closest cloud-free scene (July 14th) and field measurement date (July 31st). For two measured points we recorded water depths of 80 cm on July 31st while the July 14th scene showed exposed sandbar at the same spots (as per NDWI values and visual interpretation; Figure A4). These points on the sandbar were right at the edge of the July 14th waterline, therefore it can be reasonably inferred that the water level for the July14th scene was around 80 cm lower than the measured depths we took on July 31st (Figure A5) To account for this we subtracted 80 cm from all of the measured depths to move forward with processing of July 14th scene for bathymetry mapping.

After the depth correction we performed the Optimal Band Ratio Analysis (Legleiter et al. 2009). We extracted the pixel value for each band from each point of measured depth. We then calculated the *x* value from equation 2 for each possible band combination and plotted those values against depth in order to determine the highest R^2 value. After determining the best band combination (using R^2 value as a criteria) we used the regression formula to calculate bathymetry on the whole scene, this resulted in a bathymetry raster with values representing water depth in cm.

3.5 Results

3.5.1 Turbidity Assessment

The field measured average turbidity on August 5th 2016 was 15.4 ± 11.3 NTU (n=19) while on July 31st 2017 the river had an average turbidity of 14.5 ± 4.3 NTU (n=23). The Landsat scene from Aug 5th 2016 shows average river water NDWI values of 0.12, while the PlanetScope scene from July 14th 2017 has average river water NDWI of 0.13. Seven other cloud-free scenes from 2017 were examined for average river water NDWI values (Figure A2). From a comparison of NDWI values, visual interpretation, and preliminary bathymetry mapping tests we found that PlanetScope and Landsat exhibit clear water conditions suitable for bathymetry mapping when average water-pixel NDWI values > 0.1. Confidence levels for bathymetry mapping drop significantly if scene-average NDWI values were less than 0.1.

3.5.2 Bathymetry Mapping

Using the July 14th 2017 PlanetScope scene and 28 field measurements of water depth we performed an Optimal Band Ratio Analysis and determined that the Green and Red bands performed best in the band ratio formula. We then ran 5 iterations of measured water depths regressed against the ln(green / red) to ensure high confidence for the regression statistics. Each iteration used a different set of 21 random points for regression, saving the remaining 7 for accuracy assessment (Figure A6). See Table A1 for the R^2 values, standard errors, and Root Mean Square Error (RMSE) value associated with the five regression analyses.

The RMSE values are in cm and calculated from the 7 points set aside for accuracy assessment. To calculate RMSE we used the regression formula from each iteration to calculate

bathymetry for the whole study area, and then extracted the calculated water depth values for the 7 known depth points for RMSE calculation. Between our 5 iterations we see an average RMSE of 21.8 ± 4.7cm (Table A1).

The bathymetry equation from Iteration 2 (Figure 3.3) was used for final bathymetry mapping as it had the highest R^2 value (0.89) along with the lowest standard error (22.4 cm) of the five regressions.

$$y = 1243.2x - 46.298 \quad (4)$$

y: Depth in cm

x: ln(Green / Red)

We applied a green, yellow, red color ramp to the resulting bathymetry raster. Green represents deep water pixels (near or above 2m) while red represents shallow water pixels (Figure A7).

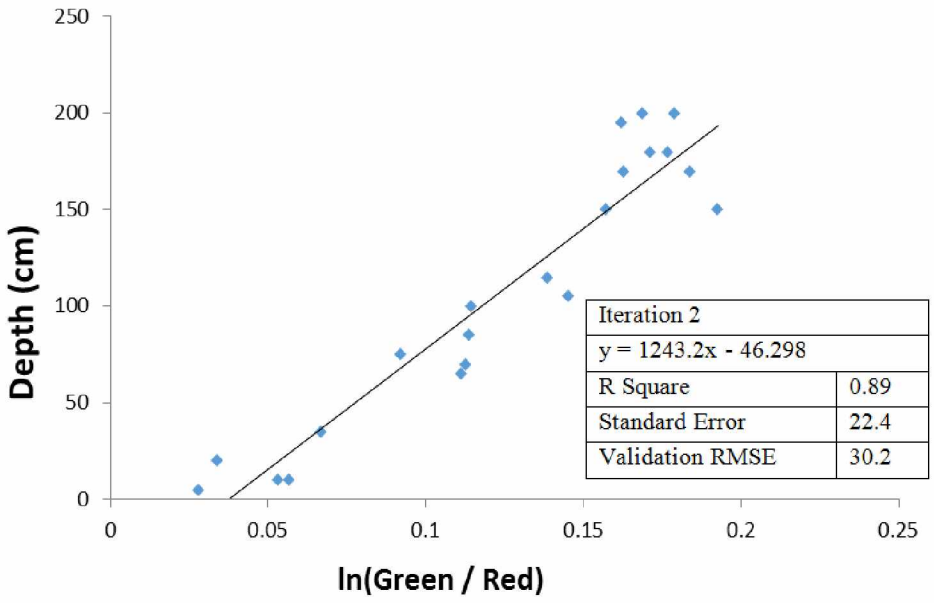

Figure 3.3. Iteration 2 scatter plot [ln (green/red) vs water depth] and regression statistics.

3.6 Discussion

Availability of a large number of images for the study area is important when assessing the feasibility of continued river bathymetry monitoring on the Colville using seasonal cloud-free images. Historically, for the June 15th – September 30th observation period, 25% of the days are

cloud-free (Weather Underground n.d.). 2016 and 2017 were above average rainfall years for Nuiqsut (it received twice as much rainfall in 2016 and 2017 compared to the average rainfall during 2010-2015) and we had 23% cloud-free days. Refer to "Expected future image availability" in the Appendix. Of these days, in 2017 we found 16 unique days of clear water conditions suitable for mapping river bathymetry (Table 3.2). Based on these findings we can reasonably assume that future years will have similar or higher number of cloud free and clear water days for bathymetry monitoring using optical images.

Table 3.2. Summer 2017 image availability statistics

Scene Availability between Jun 15th 2017 and Sep 30th 2017	
Total scenes; PlanetScope, Sentinel, Landsat	138
Total unique days imaged	88
Total number of cloud free scenes	37
Unique cloud free days imaged	25
Total number of cloud free and clear water scenes	23
Unique cloud free clear water days imaged	**16**

Heavy rain can increase surface runoff, especially in continuous permafrost zones, like our study area, where water is unable to permeate the frozen subsoil and is transferred across the surface into the river (Kuchment et al. 2000). This surface runoff carries along sediment from the loess bluffs bounding much of the river (Payne et al. 2018, Walker and Everett 1991). Because the sediment in this area is so fine grained and stays suspended in the water column longer it creates conditions of high turbidity for several days after a heavy rain event (Van Rijn 1993). On July 25th, 2017 there was a large rain event in the study area (Weather Underground n.d.) that increased water turbidity, and rendered multiple images of July 27th 2017 unsuitable for bathymetry mapping.

If future years have rainfall similar or less than what we saw in 2017, then we can expect similar or more days of clear water conditions suitable for collecting field validation data and bathymetry mapping. Multiple depth maps from a single season will also help to assess the validity-period for bathymetry products. The Colville water depth is relatively dynamic and can

change quickly (Arnborg et al. 1962, 1966). Knowing how long a depth product can remain useful will help assess the number of in season dates that need to be mapped in order to characterize the full cycle of the river from spring breakup to the fall freeze up.

For a proof of concept we successfully mapped bathymetry using a July 14th PlanetScope image. The R^2 values for water depth vs natural log of (Green/Red) ranged from 0.80 to 0.89, better than the R^2 values from similar studies (e.g. Winterbottom and Gilvear 1997, Legleiter et al. 2004, 2009, Legleiter 2013). The average RMSE of 21.8 cm (from 5 iterations) is an acceptable amount of error for the purposes of using this product to aid in river navigation. These results show promise for achieving replicable depth maps with similar levels of accuracy in the future under similar conditions. The end product could easily be distributed and integrated into a smartphone or GPS device by the user (Figure A8). Like many maps, this product would be used in tandem with the local knowledge and judgment of the boat operator (Gearhead 2010). This product will aid navigation by identifying shallow water sites, sites of interrupted channel connections, and offering a latest status of the river channel.

An end product user can rely on the bathymetry product, color depth map, generated from the July 14th scene (Figure 3.4a) to safely navigate the shallow water spots in the main channel and poorly connected side channels. We then tried to generate a visually similar product without any ground truth points or regression. The natural log of the green over red band without the regression line coefficients (m and b derived from measured depths) exhibits a similar distribution of water pixels along the color scale (Figure 3.4b). Figure 3.4a was generated from the field depth points and the regression equation from Iteration 2 shown in Figure 3.3. Figure 3.4b was generated using only the natural log of the green over the red band from July 14th image without any other inputs or ground truth data. These figures show that even without associated ground truth data, a useful product for boat navigation can still be generated. While having ground truth data is always preferred, the relative depth mapping method can make good use of all available imagery exhibiting suitable conditions for bathymetry mapping eliminating the need for ground truth water depth data.

We applied the relative depth mapping technique on PlanetScope, Sentinel, and Landsat (cloud free and clear water) scenes acquired on the same dates (June 29th and July 9th, 2017). Even though the spatial resolutions of the three sensors vary, similar patterns of water depth can

be observed on all three images for both June 29th and July 9th (Figure 3.5). Since the relative depth maps from Sentinel and Landsat show nearly identical depth patterns as the PlanetScope map, which we have already shown to be an accurate representation, we can reasonably assume that the relative depth mapping technique works for these sensors as well. It can also be safely assumed that with ground truth data similar to the July 14th PlanetScope scene, reliable bathymetry with depth values could also be calculated from Sentinel and Landsat scenes. The inclusiveness of all three sensors for mapping bathymetry adds to the feasibility for continued monitoring while at the same time making a strong case for using our technique with any optical sensor with similar bands.

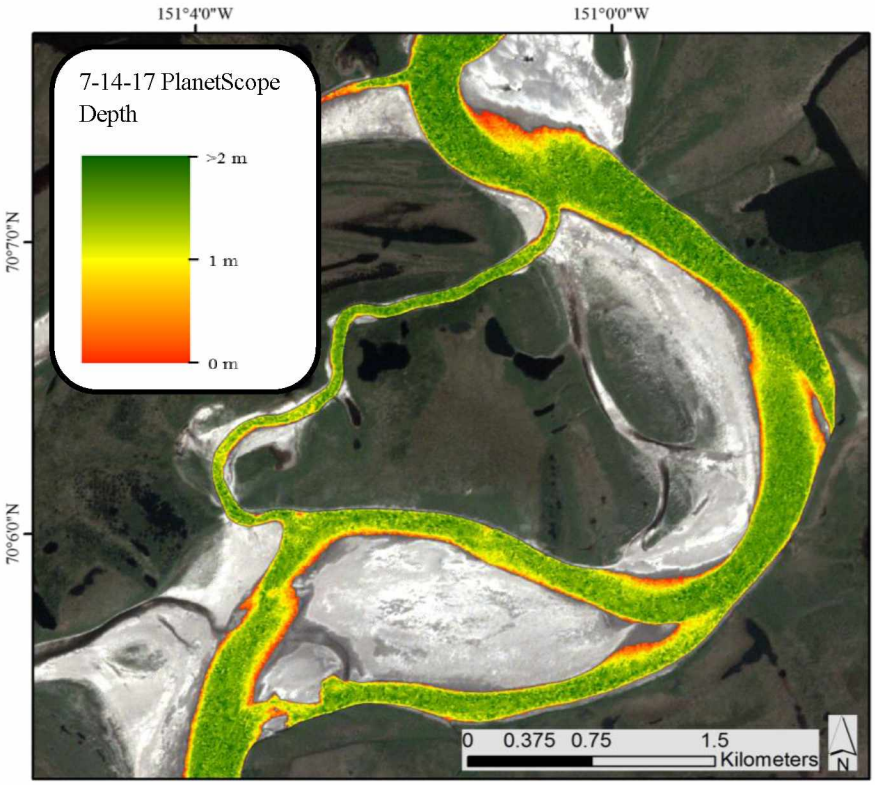

Figure 3.4a. Absolute water depth generated from July 14th PlanetScope image.

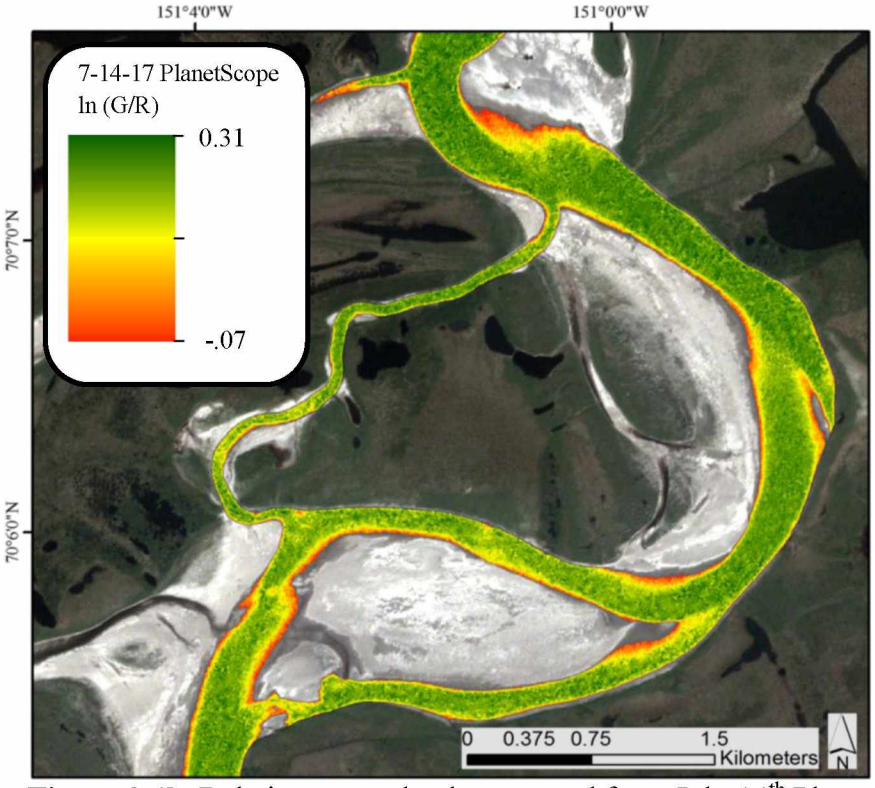

Figure 3.4b. Relative water depth generated from July 14th PlanetScope image.

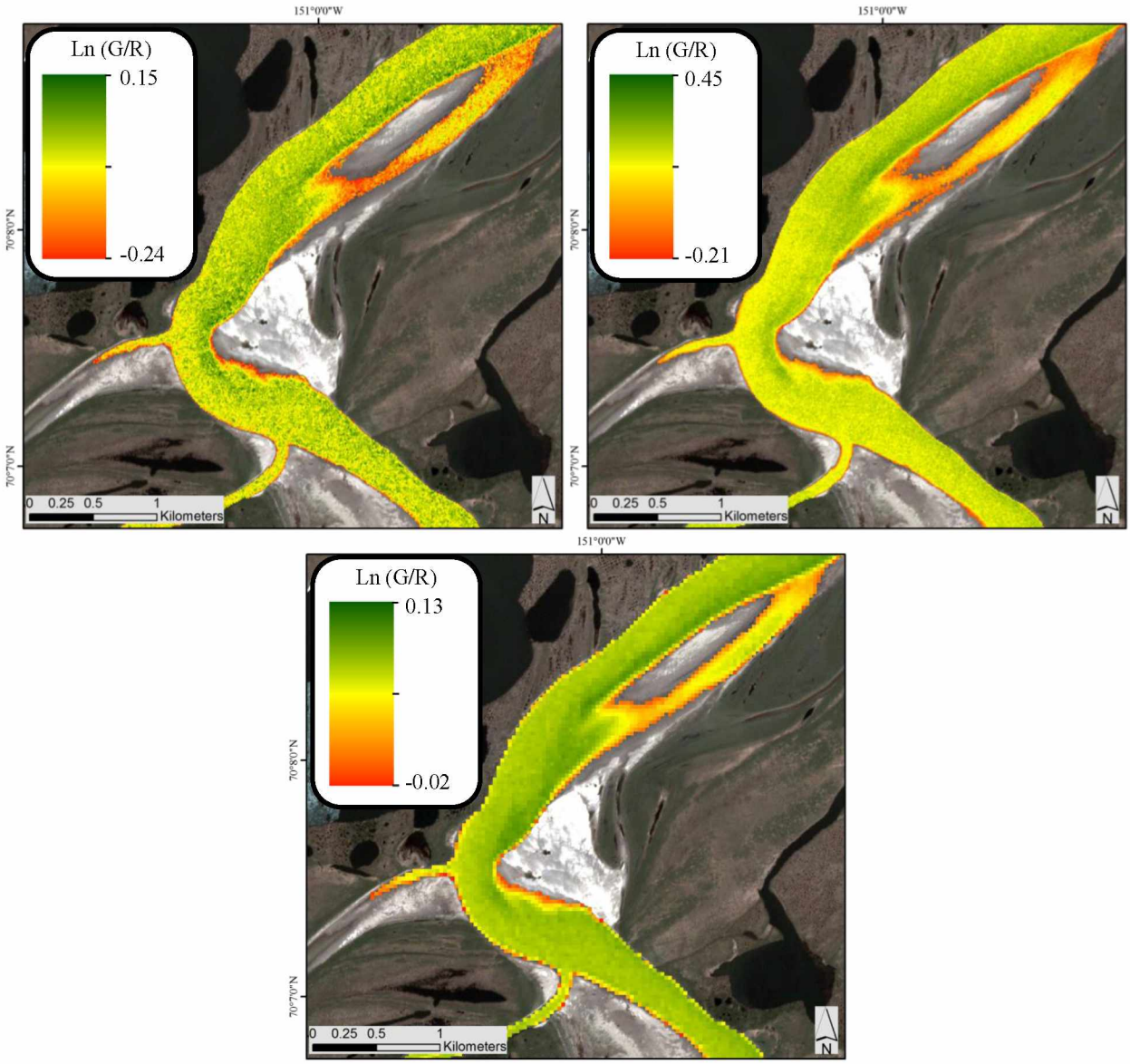

Figure 3.5. Comparison of relative depth map products derived from PlanetScope, Sentinel, and Landsat scenes from June 29th 2017

The multisensor comparison helps to determine the appropriate spatial resolution/ pixel size for mapping river bathymetry. Many river bathymetry studies focus on small rivers where a Landsat pixel may be too large to isolate river water making high resolution imagery a necessity (Winterbottom and Gilvear 1997, Legleiter et al. 2004, 2009). Our study has the advantage of working on a very large river, often greater than 600 m wide on the main channel within the

study area. This reduces the necessity of high resolution imagery (Legleiter et al. 2004) which gives the analyst freedom to determine optimal pixel size. An example of this can be observed in Figure 3.5. Because of its high spatial resolution the PlanetScope map appears grainier than Sentinel and Landsat. The Landsat map exhibits useful patterns but can be influenced along the water / land boundary by mixels, or pixels of mixed water and land (Shulong 1995), which isn't as significant an issue for PlanetScope and Sentinel. The Sentinel imagery has a large enough pixel size to avoid heavy grainy appearance, while being small enough to detect shallow water spots that may be averaged out and missed by Landsat. With this in mind the analyst has freedom to choose from a variety of pixel sizes for mapping bathymetry, and may also choose to resample higher resolution imagery to a size still useful for navigation, while avoiding a grainy appearance.

This range in pixel size availability may also prove useful for future bathymetry mapping of the Colville beyond our study area. To the direct north and south of the study area, the Colville changes in average channel width and morphology. To the north the Colville enters its delta, which empties into the Beaufort Sea. South of the study area the morphology of the river changes from a predominantly single channel to a braided channel, characterized by even shallower water conditions along with multiple channels to choose from when navigating the river. An area like this would benefit heavily from a bathymetry product, especially in identifying channel connections in order to find direct routes down and upstream. In case of narrower braided channels the user may benefit from a higher resolution depth map as opposed to our single channel study area. We also conclude that if clear skies and relatively clear-water conditions are met, remote sensing based bathymetric mapping as outlined above is feasible.

Future field data collection would further test the robustness of this technique and help transition this study from feasibility to implementation, and eventually a fully proven and developed monitoring project led by the community. This study serves as the starting point to that process by: connecting with the community, addressing their concerns with science, and assessing the feasibility of continued monitoring by using freely available image data.

3.7 Conclusion

This study assessed the feasibility of continued river depth monitoring with optical remote sensing to aid river navigation. The design and implementation of this study was done in tandem with guidance and input from the Alaska Native community of Nuiqsut. By outlining simple robust methods for mapping river bathymetry we have set a framework for continued depth monitoring.

Given similar cloud free and clear water conditions (which we have shown should happen plenty of times each summer) as well as identified tangible assessment thresholds, our technique will work in the future for mapping bathymetry relevant to navigation, with or without water depth data. This technique will work for at least three sensors and should be replicable for any optical sensor with spatial resolution ranging from 3 - 30m. More field data should help test the robustness of this method and give an idea on the average validity-period for a particular bathymetry map product. The river depth products will not only benefit the community but also build a database over time of river depths, which can provide valuable information for other studies as well as aid in planning and decision making for subsistence access issues. In conclusion, the idea of continued depth monitoring for the Colville using remote sensing is feasible using the methods presented here and could be achieved by a non-scientist with minimal remote sensing / GIS training. An implementation of our methods by the community, in order to create a river depth monitoring program, would be an important step forward for the advancement of community based science and the co-production of knowledge.

Acknowledgment

This work was supported by an Alaska NSF EPSCoR award #OIA-1208927 and the state of Alaska, as well as the Alaska Space Grant and the UAF Global Change Student Research Grant. The authors would like to thank the community of Nuiqsut especially Mr. Frederick Tukle Sr. for his generous assistance with fieldwork and Mr. James Taalak for helping us connect with other indigenous river users.

References

Alaska Native Tribal Health Consortium (ANTHC): Community observations on climate change – Arctic Village, Fort Yukon and Venetie, Alaska, 2016 63 pp.

Allouis T, Bailly JS, Pastol Y, Le Roux C. Comparison of LiDAR waveform processing methods for very shallow water bathymetry using Raman, near-infrared and green signals. Earth Surface Processes and Landforms. 2010 May 1;35(6):640-50.

Armitage D, Berkes F, Dale A, Kocho-Schellenberg E, Patton E. Co-management and the co-production of knowledge: learning to adapt in Canada's Arctic. Global Environmental Change. 2011 Aug 1;21(3):995-1004.

Arnborg L, Walker HJ, Peippo J. Suspended load in the Colville river, Alaska.. Geografiska Annaler: Series A, Physical Geography. 1962 Aug 1;49(2-4):131-44.

Arnborg L, Walker HJ, Peippo J. Water discharge in the Colville River. Geografiska Annaler: Series A, Physical Geography. 1966 Dec 1;48(4):195-210.

Braund SR, and Associates. Nuiqsut Caribou Subsistence Monitoring Project : Results of Year 8 Hunter Interviews and Household Harvest Surveys. Prepared for ConocoPhillips Alaska, Inc Anchorage, AK. 2017.

Brinkman TJ, Hansen WD, Chapin FS, Kofinas G, BurnSilver S, Rupp TS. Arctic communities perceive climate impacts on access as a critical challenge to availability of subsistence resources. Climatic Change. 2016 Dec 1;139(3-4):413-27.

Bryant RG, Gilvear DJ. Quantifying geomorphic and riparian land cover changes either side of a large flood event using airborne remote sensing: River Tay, Scotland. Geomorphology. 1999 Sep 1;29(3-4):307-21.

Charlton ME, Large AR, Fuller IC. Application of airborne LiDAR in river environments: the River Coquet, Northumberland, UK. Earth Surface Processes and Landforms. 2003 Mar 1;28(3):299-306.

Clark RK, Fay TH, Walker CL. Bathymetry calculations with Landsat 4 TM imagery under a generalized ratio assumption. Applied Optics. 1987 Oct 1;26(19):4036_1-8.

Copernicus Open Access Hub. Available online: https://scihub.copernicus.eu/ (accessed May 2018)

Dankers PJT. The behaviour of fines released due to dredging: A literature review. TU Delft, Section Hydraulic Engineering, 2002.

Davies-Colley RJ, Smith DG. Turbidity suspended sediment, and water clarity: a review. Journal of the American Water Resources Association. 2001 Oct 1;37(5):1085-101.

Flener C, Lotsari E, Alho P, Käyhkö J. Comparison of empirical and theoretical remote sensing based bathymetry models in river environments. River Research and Applications. 2012 Jan 1;28(1):118-33.

Gao J. Bathymetric mapping by means of remote sensing: methods, accuracy and limitations. Progress in Physical Geography. 2009 Feb;33(1):103-16.

Gearheard S, Aipellee G, O'Keefe K. The Igliniit project: Combining Inuit knowledge and geomatics engineering to develop a new observation tool for hunters. InSIKU: Knowing Our Ice 2010 (pp. 181-202). Springer Netherlands.

Herman-Mercer N, Schuster PF, Maracle KT. Indigenous observations of climate change in the Lower Yukon River Basin, Alaska. Human Organization. 2011 Oct 1:244-52.

Hilldale RC, Raff D. Assessing the ability of airborne LiDAR to map river bathymetry. Earth Surface Processes and Landforms. 2008 Apr 30;33(5):773-83.

Horritt MS, Bates PD. Evaluation of 1D and 2D numerical models for predicting river flood inundation. Journal of Hydrology. 2002 Nov 1;268(1-4):87-99.

Johnson N, Alessa L, Behe C, Danielsen F, Gearheard S, Gofman-Wallingford V, Kliskey A, Krümmel EM, Lynch A, Mustonen T, Pulsifer P. The contributions of community-based monitoring and traditional knowledge to Arctic observing networks: Reflections on the state of the field. Arctic. 2015 Jan 1:28-40.

Johnson I, Brinkman T, Britton K, Kelly J, Hundertmark K, Lake B, Verbyla D. Quantifying rural hunter access in Alaska. Human Dimensions of Wildlife. 2016 May 3;21(3):240-53.

Kinzel PJ, Legleiter CJ, Nelson JM. Mapping river bathymetry with a small footprint green LiDAR: Applications and challenges. Journal of the American Water Resources Association. 2013 Feb 1;49(1):183-204.

Kuchment LS, Gelfan AN, Demidov VN. A distributed model of runoff generation in the permafrost regions. Journal of Hydrology. 2000 Dec 31;240(1-2):1-22.

Legleiter CJ, Roberts DA, Marcus WA, Fonstad MA. Passive optical remote sensing of river channel morphology and in-stream habitat: Physical basis and feasibility. Remote Sensing of Environment. 2004 Dec 15;93(4):493-510.

Legleiter CJ, Roberts DA, Lawrence RL. Spectrally based remote sensing of river bathymetry. Earth Surface Processes and Landforms. 2009 Jun 30;34(8):1039-59.

Legleiter CJ. Remote measurement of river morphology via fusion of LiDAR topography and spectrally based bathymetry. Earth Surface Processes and Landforms. 2012 Apr 1;37(5):499-518.

Legleiter CJ. Mapping river depth from publicly available aerial images. River Research and Applications. 2013 Jul;29(6):760-80.

Legleiter CJ, Overstreet BT, Kinzel PJ. Sampling strategies to improve passive optical remote sensing of river bathymetry. Remote Sensing. 2018 Jun 1;10(6).

Lotsari E, Veijalainen N, Alho P, Käyhkö J. Impact of climate change on future discharges and flow characteristics of the Tana river, sub-arctic northern Fennoscandia. Geografiska Annaler: Series A, Physical Geography. 2010 Jun 1;92(2):263-84.

Lubin D, Li W, Dustan P. Maxel C, Stamnes K. Spectral signatures of coral reefs: Features from space. Remote Sensing of Environment. 2001 75: 127-137.

Lyzenga DR. Passive remote sensing techniques for mapping water depth and bottom features. Applied Optics. 1978 Feb 1;17(3):379-83.

Lyzenga DR. Remote sensing of bottom reflectance and water attenuation parameters in shallow water using aircraft and Landsat data. International Journal of Remote Sensing. 1981 Jan 1; 2(1):71-82.

Marcus WA, Legleiter CJ, Aspinall RJ, Boardman JW, Crabtree RL. High spatial resolution hyperspectral mapping of in-stream habitats, depths, and woody debris in mountain streams. Geomorphology. 2003 Sep 30;55(1-4):363-80.

McFeeters SK. The use of the Normalized Difference Water Index (NDWI) in the delineation of open water features. International Journal of Remote Sensing. 1996 May 1;17(7):1425-32.

Meadow AM, Ferguson DB, Guido Z, Horangic A, Owen G, Wall T. Moving toward the deliberate coproduction of climate science knowledge. Weather, Climate, and Society. 2015 Apr;7(2):179-91.

Michaud JP. A citizen's guide to understanding and monitoring lakes and streams, Publ. #94-149, Washington State Dept. of Ecology, Publications Office, Olympia, WA, USA (360) 407-7472, 1991.

Moerlein KJ, Carothers C. Total environment of change: impacts of climate change and social transitions on subsistence fisheries in northwest Alaska. Ecology and Society. 2012 Mar 1;17(1).

Panda SK, Whitley M. Sixty-five Years of Colville River dynamics and its impact on present river navigability near Nuiqsut, North Slope of Alaska; Alaska EPSCoR, University of Alaska Fairbanks. 2017

Payne C, Panda S, Prakash A. Remote Sensing of River Erosion on the Colville River, North Slope Alaska. Remote Sensing. 2018 Mar 5;10(3):397.

Planet Labs. Available online: https://www.planet.com/ (accessed May 2018)

Polcyn FC, Brown WL, Sattinger IJ. The measurement of water depth by remote sensing techniques. MICHIGAN UNIV ANN ARBOR INST OF SCIENCE AND TECHNOLOGY; 1970 Oct.

Shulong Z. The Classification of Remotely-Sensed Images with Mixels [J]. JOURNAL OF THE PLA INSTITUTE OF SURVEYING AND MAPPING. 1995;4.

Stumpf RP, Holderied K, Sinclair M. Determination of water depth with high-resolution satellite imagery over variable bottom types. Limnology and Oceanography. 2003 Jan 1;48(1part2):547-56.

USGS Earth Explorer. Available online: https://earthexplorer.usgs.gov/ (accessed May 2018)

Van Rijn LC. Principles of sediment transport in rivers, estuaries and coastal seas. Amsterdam: Aqua publications; 1993.

Walker DA, Everett KR. Loess ecosystems of northern Alaska: regional gradient and toposequence at Prudhoe Bay. Ecological Monographs. 1991 Feb 1;61(4):437-64.

Weather Underground. Available online: https://www.wunderground.com/weather/us/ak/nuiqsut (accessed May 2018).

White DM, Gerlach SC, Loring P, Tidwell AC, Chambers MC. Food and water security in a changing arctic climate. Environmental Research Letters. 2007 Nov 26;2(4):045018.

Whitley MA, Panda SK, Prakash A, Brinkman TJ. 2016, Impacts of Colville River dynamics on river navigability near Nuiqsut, Alaska: 1955 - present. American Geophysical Union Fall Meeting, Homer, Alaska 12-16 December, 2016. Abstract ID: GC31H-1189.

Wilson NJ, Walter MT, Waterhouse J. Indigenous knowledge of hydrologic change in the Yukon River basin: A case study of Ruby, Alaska. Arctic. 2015 Mar 1:93-106.

Winterbottom SJ, Gilvear DJ. Quantification of channel bed morphology in gravel-bed rivers using airborne multispectral imagery and aerial photography. Regulated Rivers: Research & Management. 1997 Nov;13(6):489-99.

Xu H. Modification of normalised difference water index (NDWI) to enhance open water features in remotely sensed imagery. International Journal of Remote Sensing. 2006 Jul 20;27(14):3025-33.

Chapter 3 Appendix

Data

A.1 Remote Sensing Data

We analyzed images from PlanetScope (Planet Labs), Sentinel 2 (Copernicus Open Access Hub), and Landsat 8 (USGS Earth Explorer) for the period June 15 – September 30, 2017, the main ice-free season for the Colville as well as the most heavily trafficked time period for boat travel by Nuiqsut residents (Table 3.1). All three sensors acquire images in the blue (B), green (G), red (R) and near infrared (NIR) spectral ranges. PlanetScope was selected for its high spatial (3m) and temporal resolution (daily coverage). The two sensors (2a and 2b) on Sentinel 2 together covered the study area ~ 3-5 times per week at a 10m spatial resolution. Landsat 8 covered the study area about twice per week at a spatial resolution of 30m. The range of spatial resolution (3, 10, and 30m) from these sensors offer an excellent opportunity to examine the optimal spatial resolution for mapping bathymetry at a scale useful for navigating a large river like Colville. Using three sensors also offers additional opportunities to increase temporal coverage and to test the effectiveness of multisensor data for bathymetric mapping.

A.2 Field Data

We sampled water depth and turbidity (during 7/31/2017 – 8/3/2017) at several sites along the river within the study area from very shallow (few cm) to very deep (greater than 20m). We maximized sampling at sites at or below 2m, which is the cutoff we established for defining shallow water conditions that challenge boat navigation (Allouis et al. 2010). We collected 28 measurements at or below 2m using a 3m avalanche probe with cm increments. For deeper sites we had a 20m weighted reel tape. We used a portable MicroTPW turbidimeter for turbidity measurements which gave results in Nephelometric Turbidity Units (NTU). Locations of all measurement sites were recorded with a DeLorme GPS unit (position accuracy: ±2m).

A.3 Climate Data

Climate data, specifically cloud cover and rainfall, were examined as those are the two biggest factors that affect whether a scene can be processed for reliable bathymetry. The presence of cloud cover renders processing of optical sensors useless, and heavy rain events create large amounts of runoff which increases turbidity in the river making bathymetry mapping inaccurate.

A.4 Expected Future Image Availability

The analysis of future image availability plays a vital role in telling whether continued monitoring of river bathymetry for the Colville is feasible. We used multisensor, cloud-free 2017 summer-time images for this high-latitude study site. We were interested in the number of cloudy days as well as amount of rainfall during the study period. These are the two biggest factors that affect the ability to use optical images to map bathymetry. A cloudy scene is of no use, and a cloud free scene is only useful if turbidity levels are low so that the sensor can record river bottom reflectance for bathymetry mapping. If 2017 was normal in terms of cloud cover and rainfall then we can reasonably expect a similar amount of cloud-free clear water scenes in the future years.

Our study period from June 15th 2017 – September 30th 2017 covers 107 total days. Of those 107 days we have 138 total scenes covering 88 unique days. Of our 138 scenes, 42 were PlanetScope, 59 came from Sentinel 2, and 37 from Landsat. Of those 138 total images, 37 were cloud-free which covered 25 unique days. From the 37 cloud-free scenes, 23 exhibited clear water conditions suitable for mapping bathymetry. These 23 scenes covered 16 unique days throughout the summer (Table 3.2).

In order to characterize whether 2017 was an average year in terms of weather conditions we looked at historical climate data from Nuiqsut. Historical cloud cover data shows that within our study period, any given day has about a 25% chance of having mostly clear skies (less than 50% cloud cover) (Weather Underground). This is similar to what we saw from 2017. Of our 107 total study period days we have cloud-free imagery from 25 days or about 23%.

Total rainfall within our study time period from Nuiqsut was examined for 8 years, from 2010 to 2017 (Weather Underground). Climate, especially liquid precipitation on the North Slope has been changing which is why we averaged rainfall data from recent years (Figure A9). The average rainfall for the past 8 years was 8.3 ± 2.6 cm. 2017 was an above average rainfall year with a total of 13 cm of rain between June 15th and September 30th. 2016 also had high amounts of rainfall with 12.3 cm, but before that during 2010 – 2015 the average rainfall was 7.0 ± 1.7 cm.

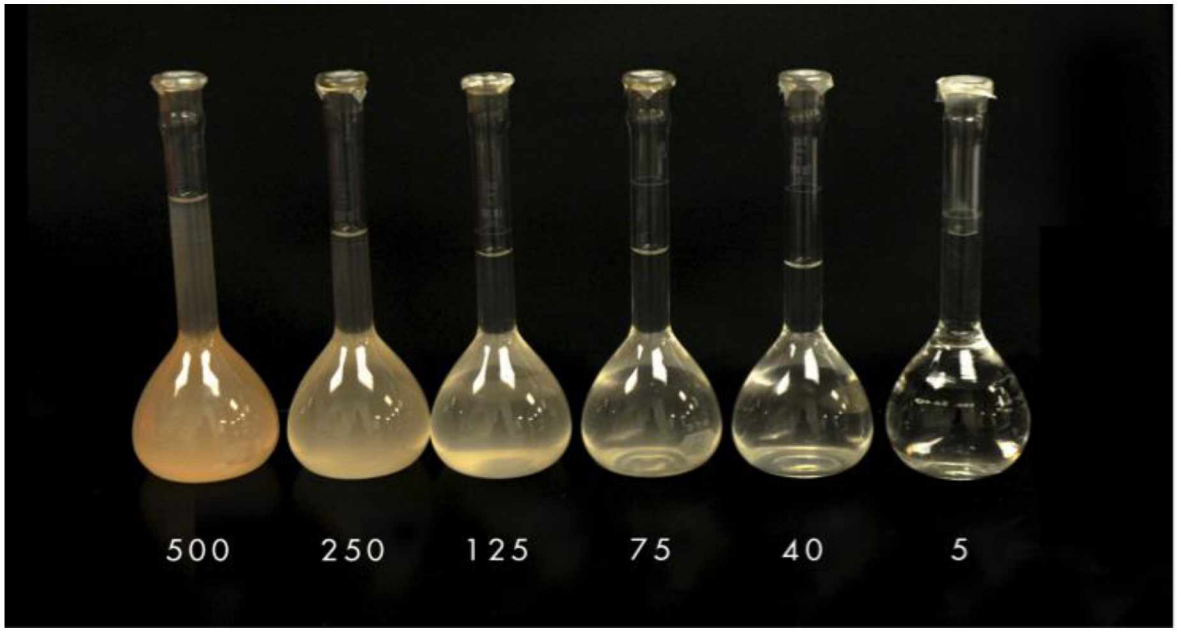

Figure A1. NTU reference guide: Image Source: https://thesummitregister.com/comparing-your-water-treatment-options-part2

Turbidity is measured in Nephelometric Turbidity Units or NTU. Figure A1 shows an example of a range of water turbidity values from 5 – 500 NTU for reference, where lower values mean clearer water and higher NTU values signify more turbid water.

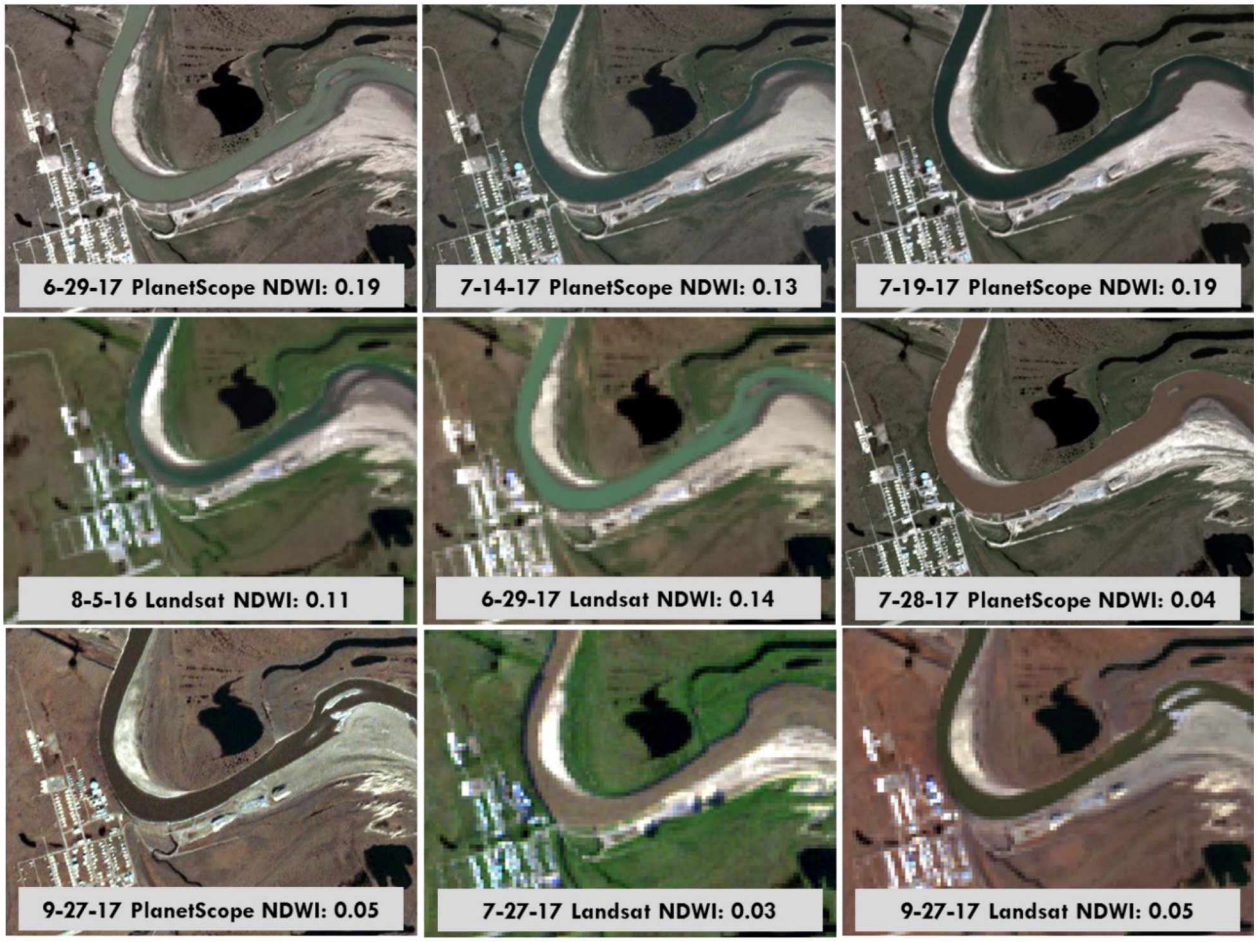

Figure A2. Comparison of 9 RGB images with calculated scene average water-pixel NDWI values.

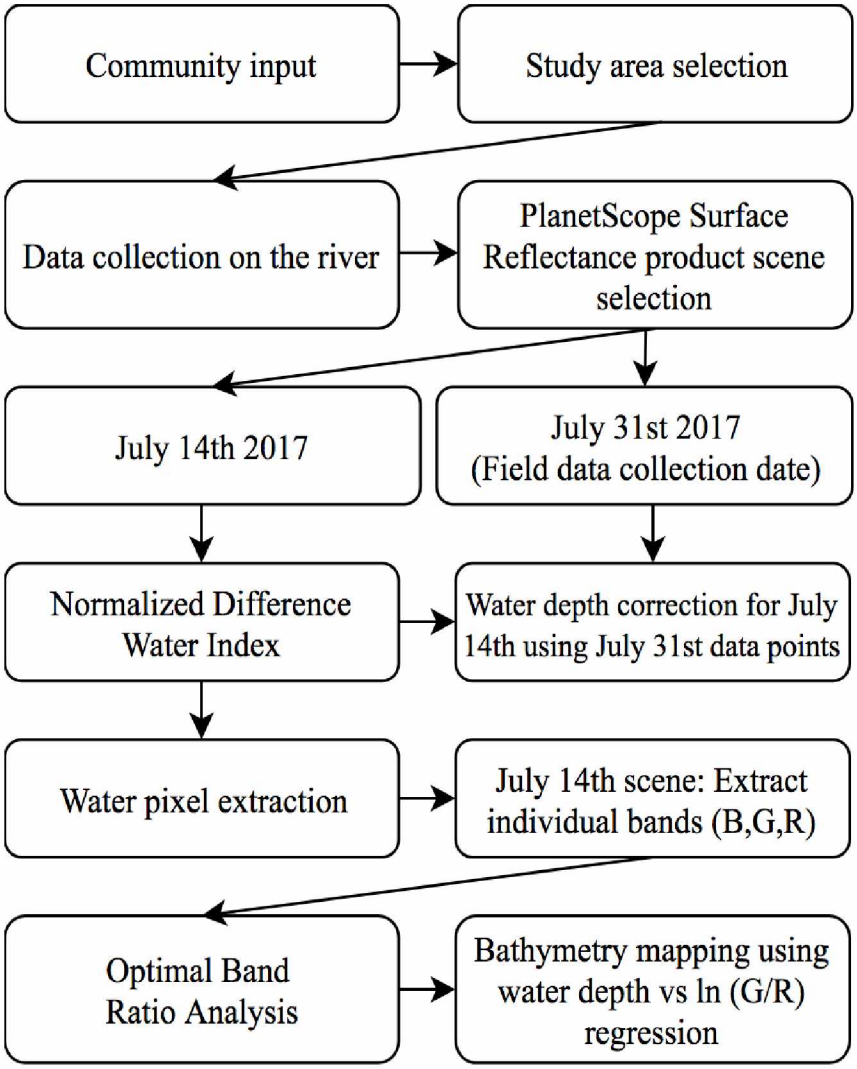

Figure A3. Bathymetry mapping workflow.

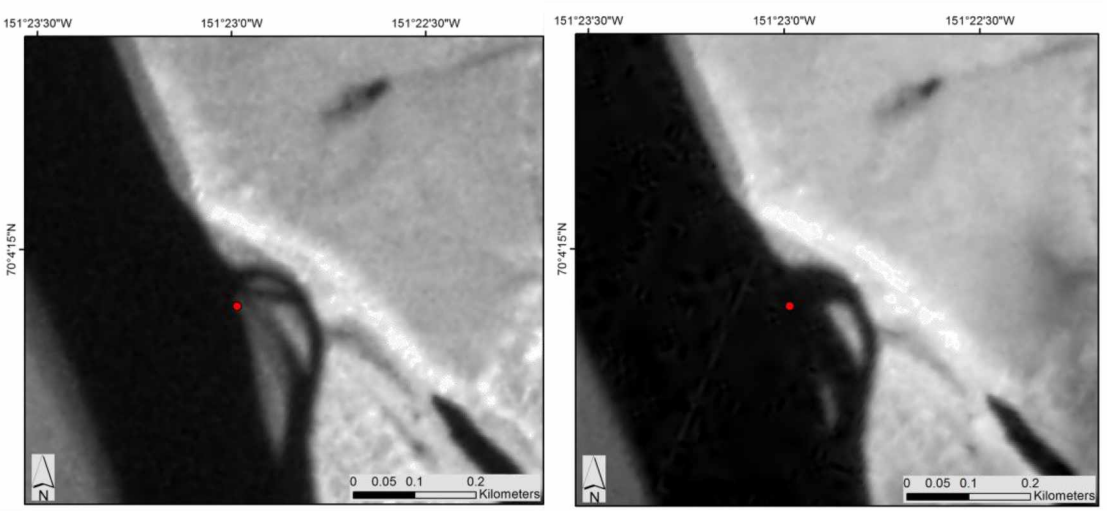

Figure A4. Comparison of water extent on 7-14-2017 (left) and 7-31-2017 (right). Red dot shows location of water depth measurement on 7-31-17. NIR bands are in the background.

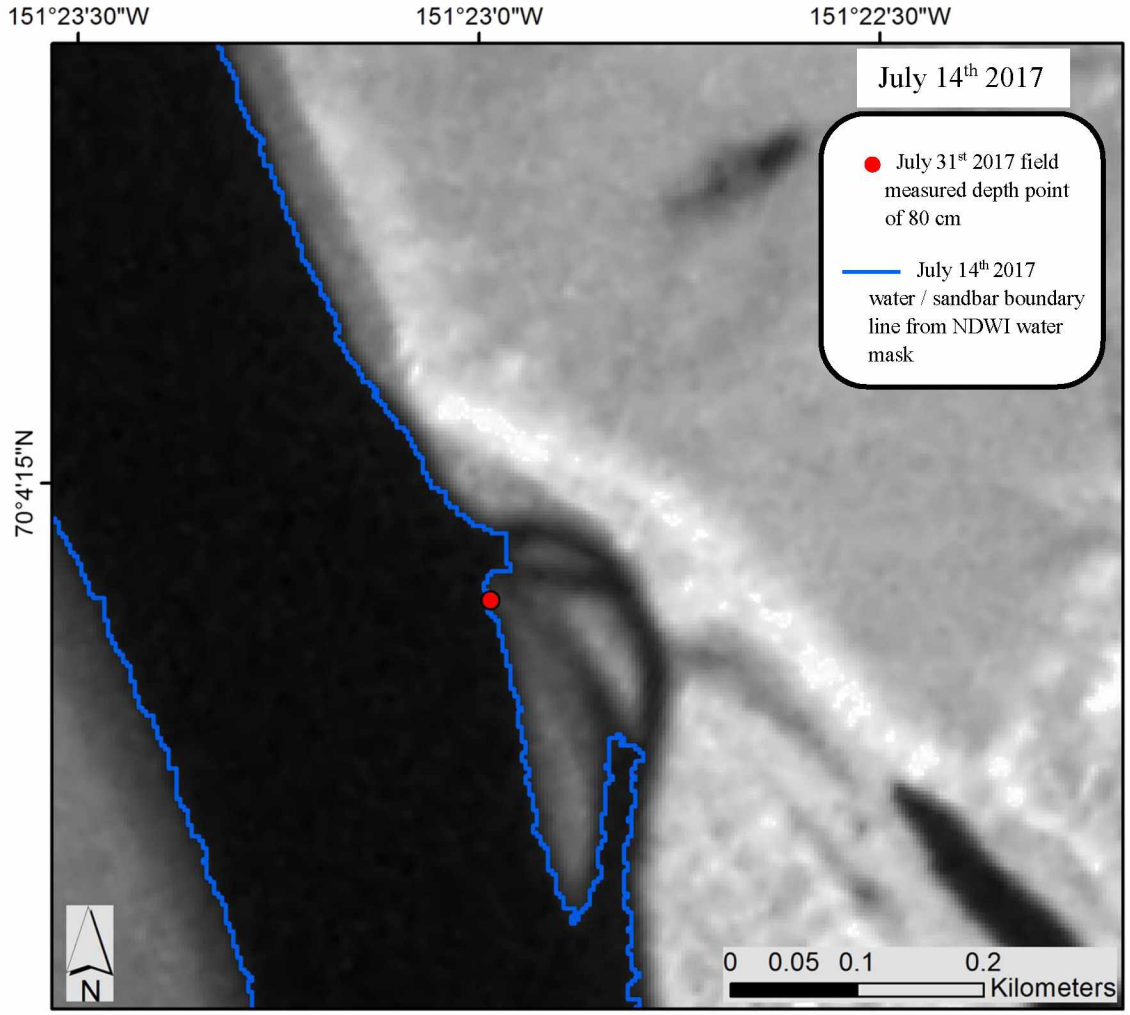

Figure A5. Water depth correction point highlighted in red, near water / land boundary of July 14th PlanetScope scene (NIR band in the background).

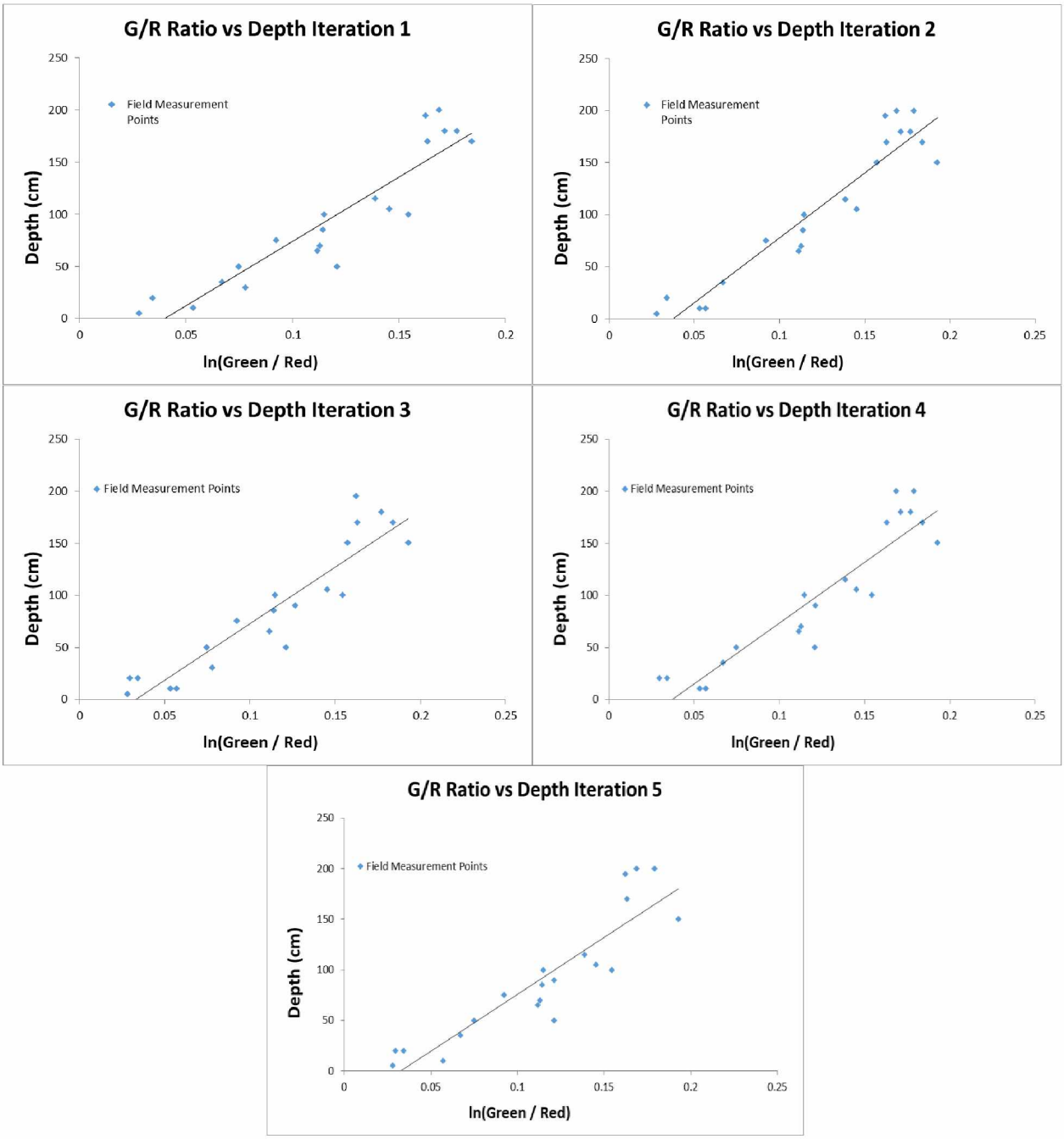

Figure A6. Regression plots from 5 iterations of our depth measurements against ln (G/R) from July 14th PlanetScope scene.

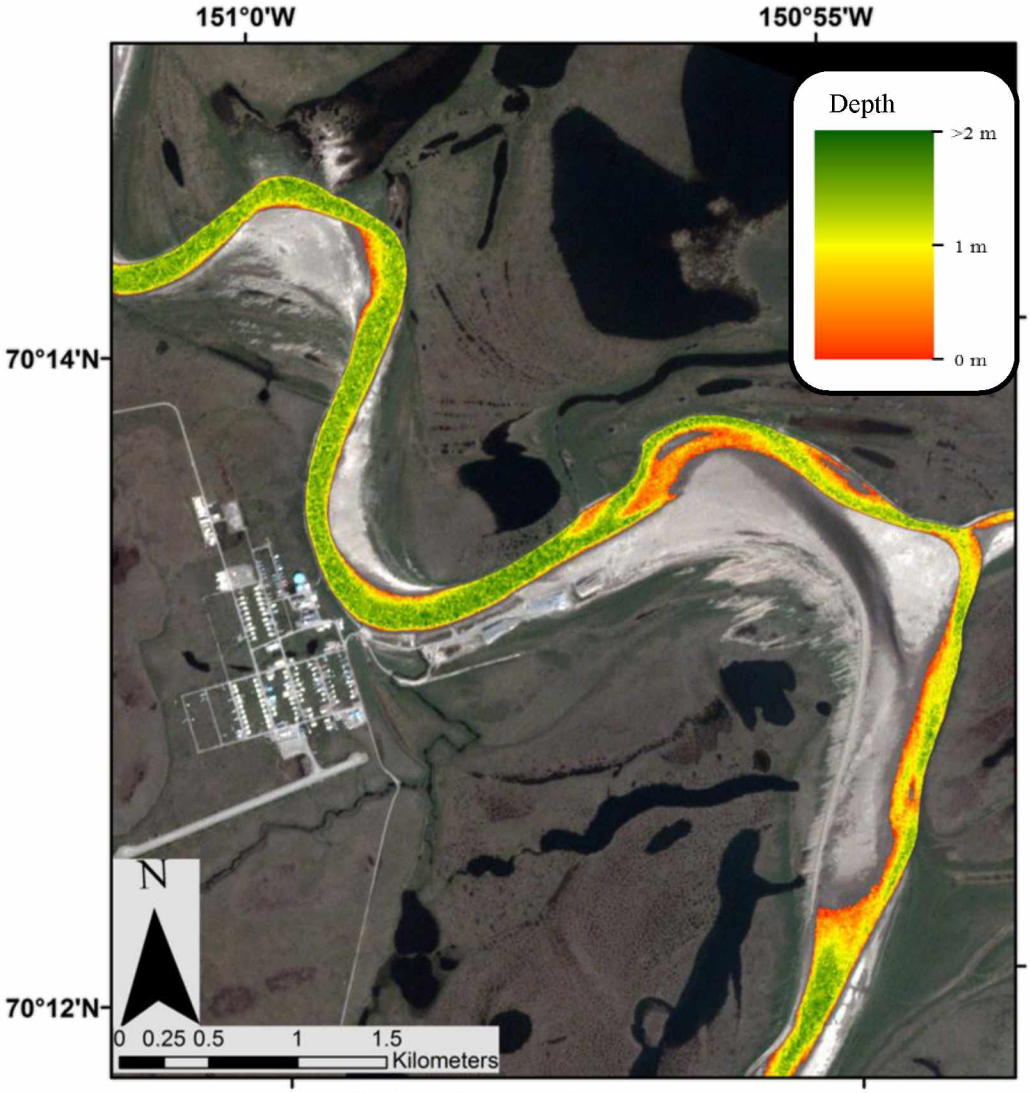

Figure A7. July 14th PlanetScope bathymetry map near Nuiqsut, overlaid on an RGB image.

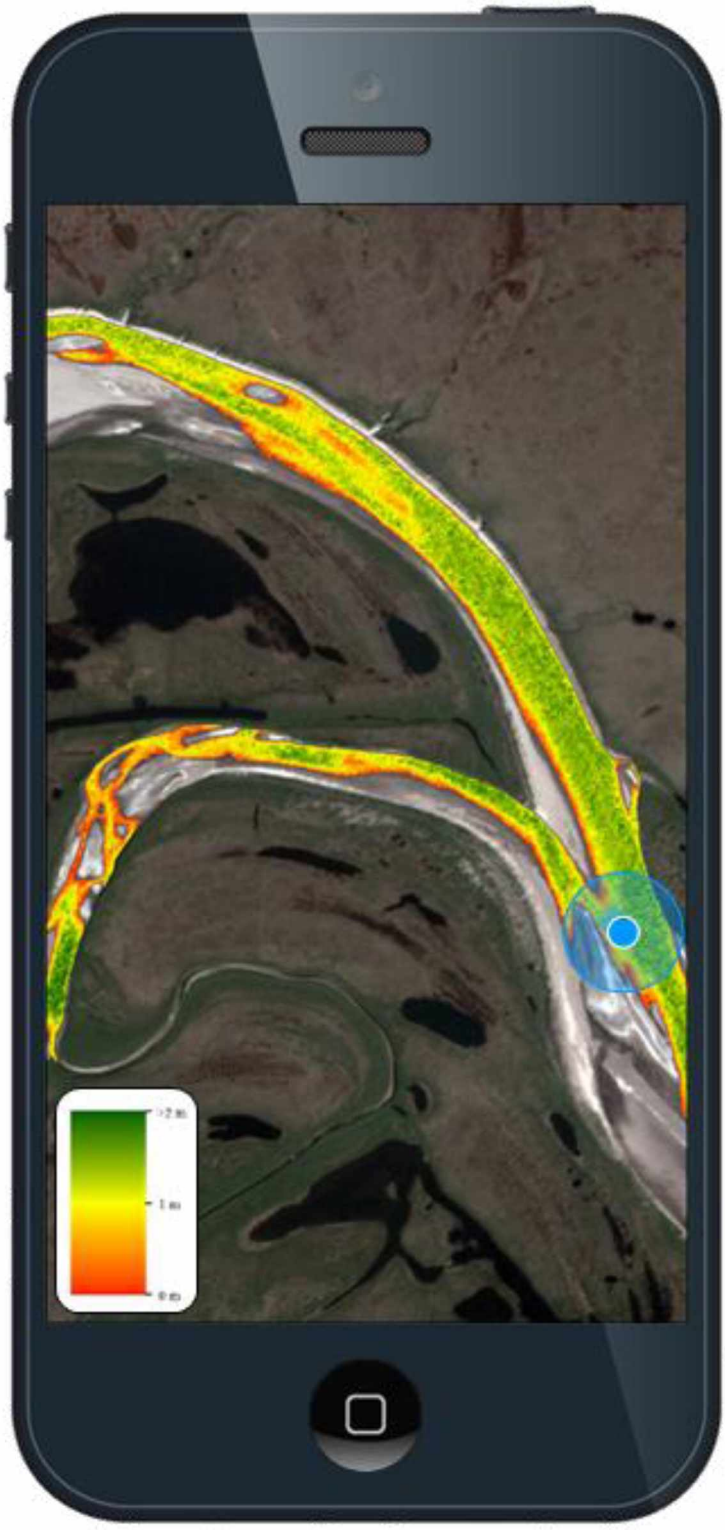

Figure A8. Example of our water depth product integrated on a smartphone.

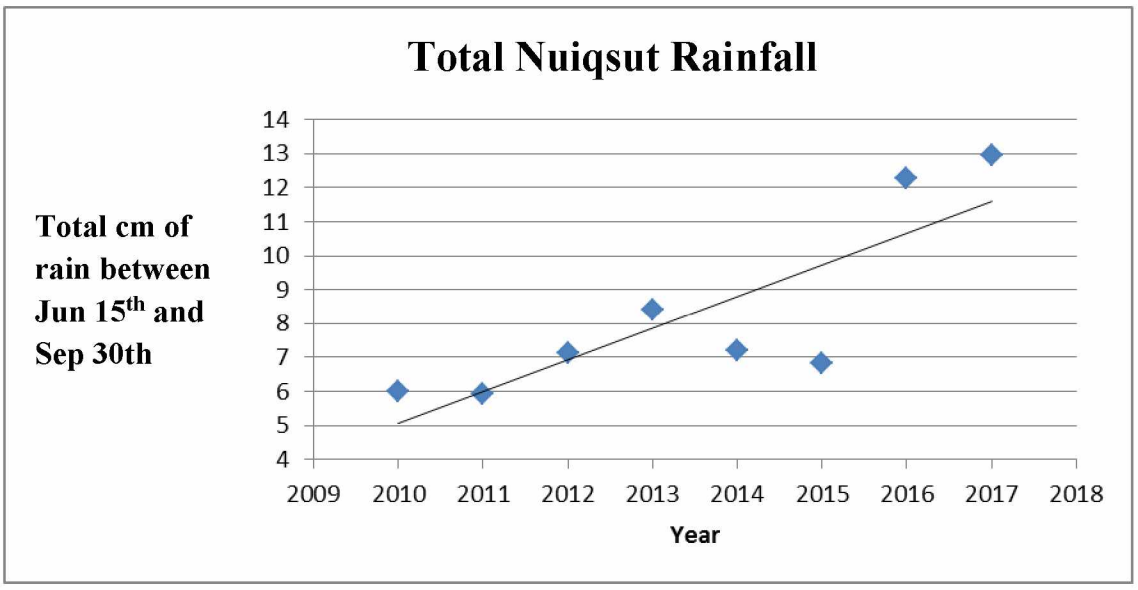

Figure A9. Total rainfall for Nuiqsut during 2010 - 2017

Table A.1. Statistics from 5 regression analyses.

Iteration 1	
y = 1236.4x - 49.49	
R Square	0.85
Standard Error	25.1
Validation RMSE	19.6

Iteration 2	
y = 1243.2x - 46.298	
R Square	0.89
Standard Error	22.4
Validation RMSE	30.2

Iteration 3	
y = 1087.1x - 35.595	
R Square	0.86
Standard Error	24.2
Validation RMSE	20.5

Iteration 4	
y = 1165.4x - 48.157	
R Square	0.86
Standard Error	25.6
Validation RMSE	22.8

Iteration 5	
y = 1124.5x - 36.591	
R Square	0.82
Standard Error	27.3
Validation RMSE	16.1

SUMMARY	
R Square Range	0.82 - 0.89
Standard Error Range	22.4 - 27.3
Avg. Validation RMSE	21.8

Chapter 4

Conclusion

For the Native Alaskan village of Nuiqsut, the Colville River serves as a main transportation artery around the North Slope of Alaska. Boat travel on the river is common for residents to reach traditional subsistence hunting sites, a practice that is vital for the nutritional needs of Nuiqsut residents. Nonetheless, there have been many reports of accelerated changes in the river environment, particularly heavy erosion and shallow channels. Heavy erosion not only threatens infrastructure and historic sites but also causes river siltation, while a shallowing channel creates hazardous conditions for boat travel. A clear need for remote monitoring of the Colville has been identified and researched in this thesis. The design and implementation of this study was done in tandem with the Native Alaskan community of Nuiqsut. For an area as remote and inaccessible as the Colville, remote sensing techniques for river monitoring are the most practical approach. By outlining simple robust methods for mapping and monitoring river erosion and shallow water bathymetry we have set a framework for continued river monitoring led by the community.

It is evident that climate change, particularly climate warming of the Arctic is affecting the Colville uniquely compared to other similar sized non-Arctic rivers (Arnborg et al. 1966, Walker et al. 2003, Payne et al. 2018). Although we discuss erosion and shallow water bathymetry separately in this thesis, we speculate that increased erosion due to climate warming is directly tied to shallowing of channels and unpredictable changes to the Colville, as reported by Nuiqsut residents.

Analysis of high-resolution satellite data indicates that bank erosion on the Colville River seems to have increased during the past 36 years (1979/1982 - 2015) compared to erosion during 1955-2015. Of four erosion sites analyzed, two showed significant increases in yearly erosional rates from 1.8 m/y to 2.2 m/y and from 0.7 m/y to 1.0 m/y for our two studied time periods. One site showed similar erosion rates of 1.6 m/y between the two time periods and a fourth site showed a decrease in erosion rates from 1.2 m/y to 0.8 m/y. However, we found out that the average erosion rates (i.e. erosion distance divided by timespan) do not necessarily provide a complete and accurate picture of the extent and severity of bank erosion. Hence, to get an

accurate understanding of the riverbank erosion process of the Colville, we not only estimated the long-term erosion rates, but also changes in erosion area and the volume of land loss. At one of the sites the difference in the erosion area was almost double, from 51,714 m^2 to 97,843 m^2 between the periods 1955 – 1979 and 1979 - 2015. At another site, the difference in the erosion area was more than double, from 23,884 m^2 to 50,352 m^2 for the same periods. When we compared the average erosion rate at one site (1.6 m/year) to another site (1.0 m/year), we saw that the former site had a much higher erosion rate. However, the latter site had the tallest banks (average bank height of 33 m) and the volume of land loss was 1,689,813 m^3 for the period 1979–2015, which was ten times more than the volume of land loss at the former site (average bank height of 5 m) for the same period.

The novelty of this erosional research is in extending the estimates from two-dimensional surface erosion rates (as reported by most studies) to three-dimensional volumes (i.e., the amount of material eroded). Whereas there is a wealth of literature available on the former, there is very little published on the latter. As per our knowledge, this is the first research that demonstrates that for an Arctic river, studies on riverbank erosion that use only erosion rate can be inaccurate and grossly conservative. This study validates the significance of mapping erosion areas and estimating land loss volumes to gain an accurate understanding of the amount and severity of riverbank erosion, as in certain areas the volume of land loss can be disproportionately higher than what average erosion rates may suggest. Hence, this study presents not only an improved understanding of the extent and severity of riverbank erosion along parts of the Colville, but also establishes a method for evaluating land loss from typical eroding banks using publicly available DEMs.

We demonstrated that high spatial resolution imagery can be effectively used to monitor bluff line erosion along Arctic rivers. This type of monitoring can enhance understanding of hydro-geomorphological processes along Arctic rivers and provide information for estimates of future change. We have also demonstrated that estimating erosion via automated change detection based on simple classification methods can be as effective as digitizing by hand. This is important for monitoring large study areas or making multiple change observations in areas where hand-digitization is not feasible. We have also successfully used a current DEM to calculate the cubic volume of past erosion, and demonstrated the efficacy of this simple method

for relatively flat Arctic regions. This method can be used in certain situations when land topography changes are minimal and no other source of data is available to gauge the height of eroded features.

Based on the erosion study results and analysis of climate data, it can be inferred that climate warming plays a role in erosion on the Colville. Air and ground temperature warming trends on the North Slope are likely the catalyst for increased erosion rates through the thawing of permafrost along river bluffs causing massive block failure. Warmer temperatures also mean longer ice-free seasons, which results in a longer period in which the river can erode. Trends of higher snow depths contribute to more meltwater during the spring breakup, which is the main period of erosion for Arctic rivers. If these climate trends continue, it can be inferred that erosion along the Colville will continue to increase, resulting in more problems for the residents of Nuiqsut, including shallowing of the river channel due to increased siltation, which is why we also assessed the feasibility of river depth monitoring with optical remote sensing, to aid river navigation.

This study assessed the feasibility of continued river depth monitoring with optical remote sensing to aid river navigation. We successfully mapped shallow water bathymetry for the 2017 ice-free season using optical images from three different sensors and a proven empirical (OBRA) method. Comparison of image derived depth values to field-measured depth values showed an average RMSE of 21.8 cm, which is an acceptable amount of error for the purpose of using image-derived bathymetry products to aid boat navigation. The end product could easily be distributed and integrated into a smartphone or GPS device. Like any map, this product should be used in tandem with the local knowledge and judgement of the boat operator.

We have shown that under cloud free and clear water conditions our technique will work for mapping bathymetry relevant to boat navigation, with or without water depth data. This technique will work for at least three sensors and should be replicable for any optical sensor with spatial resolution ranging from 3 - 30m. More field data should help test the robustness of this method and give an idea on the average validity-period for a particular bathymetry map product. The river depth products will not only benefit the community but also build a database over time of river depths, which can provide valuable information for other studies as well as aid in planning and decision making to address subsistence access issues.

Heavy erosion and shallowing of channel play into the larger scheme of river geomorphology on the Colville. Future research on remote monitoring of river bathymetry can spur new research in the related fields such as fisheries, river hydrology, permafrost, community based science, harvesters' access issues, etc.

Direct future work from this study would include continued river monitoring and the collection of more ground truth data in order to further test the robustness of our methods. We expect a continued increase in erosion along bluff sites as well as shallowing of river channels. With the recent addition of high temporal and spatial resolution satellite imagery, such as PlanetScope, continued yearly erosion and bathymetry monitoring is plausible and would be a valuable dataset for planning and decision making for the community of Nuiqsut.

Due to the scarcity of high-resolution historic image data we were able to analyze images from only four summers for the period 1955 - 2015, but recent launch of many high resolution sensors should facilitate yearly monitoring of bluff erosion along the Colville. Given the fact that Nuiqsut has critical infrastructure near the bluffs, having accurate erosion estimates will help for better planning and mitigation of potentially costly damages.

The development of a Rapid Assessment Tool (RAT) for mapping shallow channels would be a valuable dataset for boat navigation on the river as well as studying geomorphological changes both intra-seasonal and year to year on the Colville. Plans have been set in place for Nuiqsut residents to collect additional sets of depth measurements from summer 2018. This can easily be performed with existing technology residents already use, such as boat depth finders and handheld GPS units. Having this additional dataset would allow further validation of our methods and estimating error on the image-derived bathymetry products. Ideally we would see accuracies similar to that of our 2017 imagery, with an emphasis on highlighting potential shallow water sites and channel connections. Multiple dates from one summer season should also be processed in order to see the length of validity of one depth product, thus giving an idea of how many scenes need to be processed in one season to fully characterize geomorphological changes.

In conclusion, the idea of continued river monitoring for the Colville using remote sensing is feasible using the methods presented here and could be achieved by a non-scientist

with minimal remote sensing / GIS training. An implementation of our methods by the community, in order to create a river depth monitoring program, would be an important step forward for the advancement of community based science and the co-production of knowledge. Furthermore, our technique may help address emerging environmental and societal issues in other regions where sufficient river navigation fosters local livelihoods.

References

Arnborg, L.; Walker, H.J.; Peippo, J. Water discharge in the Colville River. *Phys. Geogr.* **1966**, 48, 195–210.

Bird, K. J. The framework geology of the North Slope of Alaska as related to oil - source rock correlations. In Alaska North Slope oil-rock correlation study: analysis of North Slope crude. *American Association of Petroleum Geologists, Studies in Geology*, **1985**, No. 20, 3-29.

Black R. F. Gubik formation of Quaternary age in northern Alaska. *US Government Printing Office*; **1964**, Vol. 302.

Black, R. F.; Barksdale, W.L. Oriented lakes of northern Alaska. *Jour. Geology* **1949** v. 57, No. 2, 105-118.

Brinkman, T.; Hansen, W.; Chapin, F.; Kofinas, G.; BurnSilver, S.; Rupp, T. Arctic communities perceive climate impacts on access as a critical challenge to availability of subsistence resources. Climatic Change. **2016**, 139(3-4), 413-27.

Brubaker, M.; Bell, J.; Dingman, H.; Itta, M.; Kasak, K. Climate Change in Nuiqsut, Alaska, Strategies for Community Health; Publication of the Center for Climate and Health, Alaska Native Tribal Health Consortium: Anchorage, AK, USA, 2014; Available online: http://www.north-slope.org/assets/images/uploads/ANTHC_Nuiqsut_7-31-14_web_FINAL.pdf (accessed on 18 January 2018).

BurnSilver, S.; Magdanz, J.; Stotts, R.; Berman, M.; Kofinas, G. Are mixed economies persistent or transitional? Evidence using social networks from Arctic Alaska. *Am. Anthropol.* **2016**, 118, 121–129.

Carmen, G. T.; Hardwick, P. Geology and regional setting of the Kuparuk oil field, Alaska. *American Association of Petroleum Geologists Bulletin*, **1983**, 67: 1014 - 1031.

Carter, D.; Galloway, J.; Engineering Geologic Map of the Harrison Bay Quadrangle, Alaska. [Map] US Geological Survey, Washington D.C., **2005**.

Detterman, R. L. Mesozoic sequence in Arctic Alaska. *Arctic geology. American Association of Petroleum Geologists,* **1973**, Memoir 19, 376-387.

Frederiksen, N.O.; Ager, T.A.; Edwards, L.E. Palynology of Maastrichtian and Paleocene rocks, lower Colville River region, North Slope of Alaska. *Canadian Journal of Earth Sciences*, **1987**, *25*(4), 512-527.

Gross, J.; Goetz, S.; Cihlar, J. Application of remote sensing to parks and protected area monitoring: Introduction to the special issue. *Remote Sensing of Environment*, **2009**, *113*(7), 1343-1345.

Gryc, G.; Tailleur, I. L.; Brosge, W. P. Geologic framework of the "North Slope" Petroleum Province. *United States Geological Survey*, Open-file Report **1969**, 1313.

Jamison, H. C.; Brockett, L. D.; Mcintosh, R. A. Prudhoe Bay-10-year perspective. In Giant oil and gas fields of the decade 1968 - 1978. *American Association of Petroleum Geologists*, **1980**, Memoir 30, 289 -314

Kennedy, R.; Townsend, P.; Gross, J.; Cohen, W.; Bolstad, P.; Wang, Y.; Adams, P. Remote sensing change detection tools for natural resource managers: Understanding concepts and tradeoffs in the design of landscape monitoring projects. *Remote sensing of environment*, **2009**, *113*(7), 1382-1396.

Leffingwell, E. The Canning River region, northern Alaska. *US Government Printing Office*, **1919**.

Legleiter, C. J.; Roberts, D. A.; Lawrence, R. L Spectrally based remote sensing of river bathymetry. *Earth Surface Processes and Landforms*, **2009**, *34*(8), 1039-1059.

Morgridge, D. L.; Smith, W. Geology and discovery of Prudhoe Bay field, eastern Arctic Slope, Alaska. In Stratigraphic oil and gas fields-classification, exploration methods, and case histories. *American Association of Petroleum Geologists*, **1972**, Memoir 16, 489-501.

Nadasdy, P.; The politics of TEK: Power and the" integration" of knowledge. *Arctic Anthropology*. **1999**,1-8.

Payne, C.; Panda, S.; Prakash, A. Remote Sensing of River Erosion on the Colville River, North Slope Alaska. *Remote Sensing*, **2018**, *10*(3), 397.

Philipson, P.; Lindell, T.; Can coral reefs be monitored from space?. *Ambio: A Journal of the Human Environment*, **2003**, *32*(8), 586-593.

Porter, J.; Xie, L.; Challinor, AJ.; Cochrane, K.; Howden, S.; Iqbal, M.; Lobell, DB.; Travasso, M.; Netra Chhetri, N.; Garrett, K.; Ingram, J. Food security and food production systems. **2014**, 485-533

Stow, D.; Niphadkar, M.; Kaiser, J. MODIS-derived visible atmospherically resistant index for monitoring chaparral moisture content. *International Journal of Remote Sensing*, **2005**, *26*(17), 3867-3873.

Stroeve, J.; Markus, T.; Boisvert, L.; Miller, J.; Barrett, A. Changes in Arctic melt season and implications for sea ice loss. *Geophys. Res. Lett.* **2014**, *41*, 1216–1225

USGS Climate and Active Layer Data. Available online: https;//pubs.usgs.gov/ds/812/introduction.html (accessed on 18 January 2018)

Walker, H. J.; Hudson, P. F. Hydrologic and geomorphic processes in the Colville River delta, Alaska. *Geomorphology*, **2003**, *56*(3-4), 291-303.

Walker, J.; Arnborg, L.; Peippo, J. Riverbank erosion in the Colville delta, Alaska. *Geografiska Annaler: Series A, Physical Geography*, **1987**, *69*(1), 61-70.

Wendler, G.; Moore, B.; Galloway, K. Strong temperature increase and shrinking sea ice in Arctic Alaska. *Open Atmos. Sci. J.* **2014**, *8*, 7–15.